Identifying landscape hot and cold spots of soil GHG fluxes by combining field measurements and remote sensing data

Authors: Elizabeth Gachibu Wangari[1], Ricky Mwangada Mwanake[1], Tobias Houska[2], David Kraus[1], Gretchen Maria Gettel[3,4], Ralf Kiese[1], Lutz Breuer[2,5], Klaus Butterbach-Bahl[1,6]

[1]Karlsruhe Institute of Technology, Institute for Meteorology and Climate Research, Atmospheric Environmental Research (IMK-IFU), Kreuzeckbahnstrasse 19, Garmisch-Partenkirchen 82467, Germany

[2]Institute for Landscape Ecology and Resources Management (ILR), Research Centre for BioSystems, Land Use and Nutrition (iFZ), Justus Liebig University Gießen, 35392 Gießen, Germany

[3]IHE Delft Institute for Water Education, Westvest 7, 2611 AX Delft, The Netherlands.

[4]Department of Ecoscience, Lake Ecology, University of Aarhus, Aarhus Denmark

[5]Centre for International Development and Environmental Research (ZEU), Justus Liebig University Giessen, Senckenbergstrasse 3, 35390 Giessen, Germany

[6]Pioneer Center Land-CRAFT, Department of Agroecology, University of Aarhus, C. F. Møllers Allé 4, Building 1120, Aarhus 8000, Denmark

Correspondence to: Klaus Butterbach-Bahl (klaus.butterbach-bahl@agro.au.dk)

Keywords: Soil respiration, Ecosystem respiration, Methane uptake, Nitrous oxide fluxes, Random forest algorithm, Upscaling, Arable, Grassland, Forest

Abstract

Upscaling chamber measurements of soil greenhouse gas (GHG) fluxes from points to landscape scales remain challenging due to high variability of fluxes in space and time. This study measured GHG fluxes and soil parameters at selected point locations (n=268), thereby implementing a stratified sampling approach on a mixed land-use landscape (~5.8 km^2). Based on these field-based measurements and remotely-sensed data on landscape and vegetation properties, we used Random Forest (RF) models to predict GHG fluxes at a landscape scale (1 m resolution) in summer and autumn. The RF models combining field-measured soil parameters and remotely-sensed data outperformed those with field-measured predictors or remotely-sensed data alone. Available satellite data products from Sentinel-2 on vegetation cover and water content played a more significant role than attributes derived from a digital elevation model, possibly due to their ability to capture both spatial and seasonal changes of ecosystem parameters within the landscape. Similar seasonal patterns of higher soil/ecosystem respiration (SR/ER-CO_2) and nitrous oxide (N_2O) fluxes in summer and higher methane (CH_4) uptake in autumn were observed in both the measured and predicted landscape fluxes. Based on the upscaled fluxes, we also assessed the contribution of hot spots to total landscape fluxes. The identified emission hot spots occupied a small landscape area (7 to 16%) but accounted for up to 42% of the landscape GHG fluxes. Our study showed that combining remotely-sensed data with chamber measurements and soil properties is a promising approach for identifying spatial patterns and hot spots of GHG fluxes across heterogeneous landscapes. Such information may be used to inform targeted mitigation strategies at landscape-scale.

1. Introduction

Atmospheric concentrations of greenhouse gases (GHGs) such as carbon dioxide (CO_2), methane (CH_4), and nitrous oxide (N_2O) have increased since the 1750s, substantially driving global climate change (IPCC, 2019). Soils are key contributors to these GHG fluxes, with recent global emissions of approximately 350 Pg CO_2 equivalents per year (Oertel et al., 2016). Soil GHG emissions have accelerated due to human activities such as land use change for agricultural land expansion (Dhakal et al., 2022). Globally, agricultural soils are significant sources, accounting for about 37% of the GHG emissions within the agricultural sector (Tubiello et al., 2013). However, the estimates of soil GHG fluxes are highly uncertain since soil properties, land use, and land management, which are key indirect drivers of the emissions, largely differ across landscapes and regions. For instance, global annual estimates range widely from 67 to 101 Pg C (Jian et al., 2018) for soil respiration, 2.5 – 6.5 Tg N_2O-N for annual soil N_2O emissions (Tian et al., 2020), and 12 – 60 Tg for soil CH_4 uptake rates (Dutaur & Verchot, 2007). These uncertainties make it difficult to accurately quantify the GHG source or sink strengths of soils and to develop targeted mitigation options across scales.

Current upscaling approaches from localized measurements of soil GHG fluxes to landscape or regional scales using chamber or site-specific micro-meteorological methods such as eddy-covariance (e.g., Sundqvist et al., 2015; Warner et al., 2019; Vainio et al., 2021; Han et al., 2022), fail to capture the spatio-temporal variation of hot- or cold-spots, resulting in uncertainties in regional and global GHG estimates (Hagedorn & Bellamy, 2011; Levy et al., 2022). Contrary to the eddy-covariance method, chamber-based approaches can be used to capture fine-scale spatial variabilities of soil GHG fluxes within landscapes, e.g., when measurements are conducted at sampling sites representative of the spatial heterogeneities related to land use, land management, and topography (e.g., Warner et al., 2019; Vainio et al., 2021; Wangari et al., 2022). However, the ability of chambers to accurately quantify landscape fluxes over relatively larger areas is limited and closely related to the number of chamber measurement locations per unit area (Wangari et al., 2022). Previous studies have shown that the uncertainties in landscape-scale fluxes from chamber measurements using area-weighted averages increase exponentially with a decrease in the number of chamber measurement locations (e.g., Arias-Navarro et al., 2017; Wangari et al., 2022). Nevertheless, the practicality of increasing the number of chamber measurement locations to quantify landscape fluxes is constrained by extensive human and technical resource requirements, hence, there is a need for alternative ways of estimating GHG landscape fluxes.

The limitation of extensive chamber measurements required to quantify landscape fluxes can be overcome through modeling approaches that offer cost-effective and more practical alternatives. Machine learning (ML) algorithms are increasingly used to gap-fill spatio-temporal datasets on soil GHG fluxes as they require less computational time and expertise than complex biophysical models (Dorich et al., 2020; Zhang et al., 2020; Saha et al., 2021; Adjuik & Davis, 2022; Joshi et al., 2022). Amongst the available ML algorithms, the random forest (RF) algorithm has been evaluated as one of the best for predicting soil GHG fluxes (Hamrani et al., 2020; Adjuik & Davis, 2021; Han et al., 2022). The RF algorithm has been widely applied to gap-fill and upscale soil GHG fluxes in temperate ecosystems from point measurements to larger scales (e.g., Philibert et al., 2013; Räsänen et al., 2021; Vainio et al., 2021).

Several studies have explored the use of high-resolution remote-sensing (RS) datasets such as digital elevation models (DEMs) and indices from spectral characteristics derived from satellite images in combination with on-site chamber measurements to predict landscape GHG fluxes (e.g., Sundqvist et al., 2015; Warner et al., 2019; Vainio et al., 2021; Räsänen et al., 2021). These studies used RS datasets on landscape and vegetation parameters as proxies for soil physical and chemical characteristics such as soil moisture, soil vegetation cover, and nutrient availability, i.e., key biogeochemical drivers of soil GHG fluxes. However, the above studies have either been conducted over relatively small areas or have focused on individual land uses and GHG fluxes. For instance, only one study has applied a RF approach to predict CH_4 fluxes for a larger (12.4 km^2) peatland-forested landscape based on RS data and 279 on-site measurements of soil temperature, moisture, and vegetation (Räsänen et al., 2021). In addition, spatial CO_2 and CH_4 fluxes have been predicted for relatively small (~0.1 km^2) forested landscapes using DEM-derived terrain attributes and a few site-measured (temperature and moisture) soil variables (Warner et al., 2019; Vainio et al., 2021). Applying RF models using various RS datasets and soil parameters for soil GHG flux predictions on larger and heterogeneous landscapes in relation to land use, topography, and soil conditions remains unexplored. It is still uncertain whether such landscape flux predictions would improve if supplemented by multiple actual field measurements of soil properties (e.g., texture) and variables (e.g., inorganic N content), which may better describe the geochemical and physical conditions compared to RS-derived indices.

In this study, we aimed to determine the potential of applying the RF algorithm to predict the spatial and seasonal variability of soil CO_2, CH_4, and N_2O fluxes using a high number of stratified sampling locations (n = 268) spread across a relatively large (~5.8 km^2) landscape with heterogeneous land uses (forest, grassland, and arable land). Specifically, we: (a) evaluated the effectiveness of high-resolution RS data and relatively low-resolution data on soil physico-chemical parameters in predicting soil GHG fluxes across different land uses; (b) predicted high-resolution soil GHG fluxes at a landscape scale and detected GHG hot spots and cold spots; and (c) compared landscape GHG fluxes upscaled from RF-predicted high-resolution maps with aggregated landscape flux estimates from averaged (point) fluxes multiplied by landscape area. We hypothesized that combining RS data that act as proxies of key drivers of soil GHG fluxes (e.g., vegetation cover and water content) and site-measured soil parameters representing the actual field conditions would yield improved GHG flux prediction accuracies in our models than using either RS data or site-measured soil parameters in isolation. We expected fine-scale hot spots (within a few meters) to occur in cultivated areas and cold spots in forested areas. We also hypothesized that the high-resolution upscaled fluxes, which represent most GHG hot and cold spot regions across the landscape, would avoid possible under- or overestimations of landscape fluxes derived from land use specific area-weighted averages calculated from few point chamber measurement locations.

2. Materials and methods

2.1 Study area

The study area is located within the Schwingbach catchment in Hesse, central Germany (50°30'4.23. N, 8°33'2.82. E). The landscape covers an area of approximately 5.8 $km^{2,}$ excluding the human settlement areas and road networks. Land uses within the landscape are mainly forests (57%) and arable lands (34%). Grasslands cover about 8% and are primarily located in riparian zones. The forest is mainly covered with mixed (44%) trees, 32% deciduous, and 23% coniferous trees (Figure 1a). The common species in the forest include European beech (*Fagus sylvatica*), spruce (*Picea abies*), European oak (*Quercus robur),* and Scots Pine (*Pinus sylvestris*) (Wangari et al., 2022). The dominant soil types (World Reference Base classification) are cambisol (69%, forest and arable), stagnosol (23%, mainly arable), and gleysol (5%), which are found along grassland riparian zones (Wangari et al., 2022). The topsoils (0 – 5 cm) in the arable and grasslands have a silt loam texture, while the topsoils in the forest land mostly have a sandy loam texture (Sahraei et al., 2020). The landscape has an average slope of 5% with an elevation range of 233 – 415 m a.s.l. The region has a temperate oceanic climate (Cfb, Köppen climate classification) with annual average precipitation and temperature of 623 mm and 9.6°C based on long-term data (1969 – 2019) (Sahraei et al., 2021).

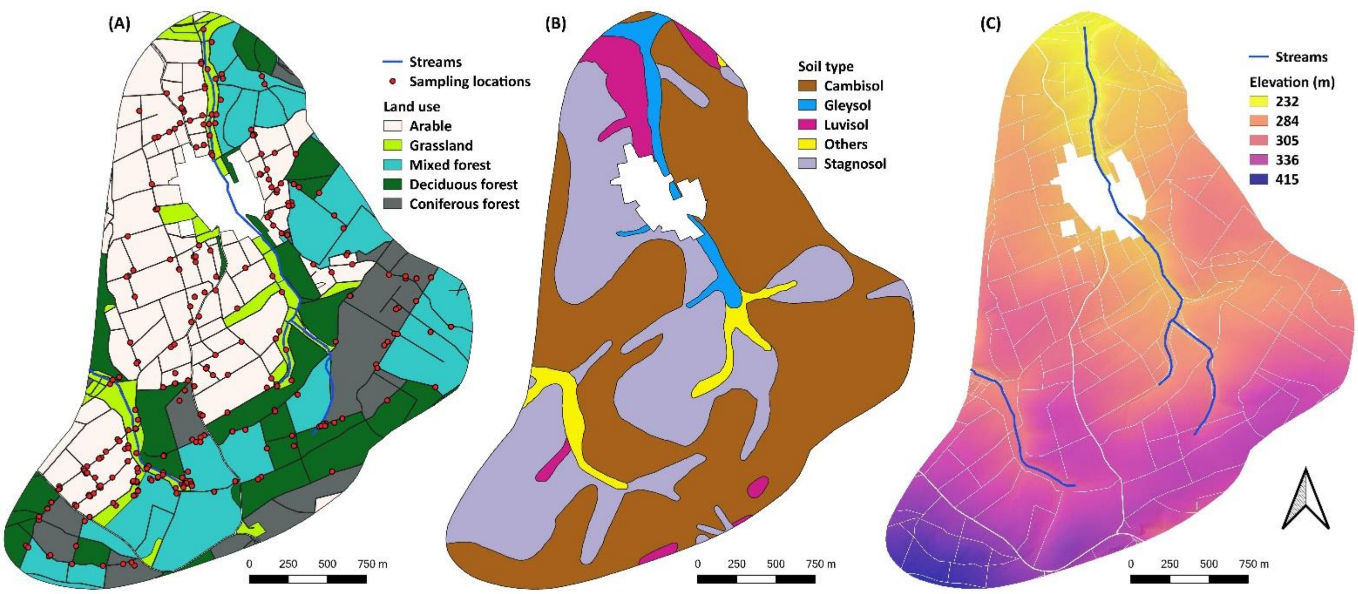

Figure 1: Map showing (a) the land uses and the location of the stratified sampling sites (selected based on combined classes of land use, slope, and soil type) across the study area; (b) the soil types (source: geoportal Hessen, https://www.geoportal.hessen.de/*)*; and (c) the digital elevation model (DEM; 1 m resolution) of the landscape (source of DEM: Hessische Verwaltung für Bodenmanagement und Geoinformation, https://hvbg.hessen.de/).

2.2 Soil physico-chemical parameters and GHG fluxes

2.2.1 Point measurements

Soil sampling and GHG flux measurements (CH_4, N_2O, and CO_2) were conducted at spatially distributed sampling sites across the study landscape (see Tab. 1 for a list of observed variables). We used a stratified random sampling approach to distribute 270 sites across different land uses (forest, grassland, and arable), soil types (cambisol, stagnosol/gleysol, and luvisol), and slopes (0–5, 6–11, and >11%) to capture the spatial variability of soil GHG fluxes and the driving parameters (Wangari et al., 2022). Out of the 270 targeted locations, field measurements were conducted at 246 sites in the summer (30th June – 9th July, field measuring campaign 1) and 268 sites in the autumn (8th – 17th September, field measuring campaign 2) of 2020. The estimated number of measured points for the forest, grassland, and arable ecosystems was ~25, 150, and 28 per km^2 (Table 1). We allocated more grassland sites due to the hypothesis that riparian grasslands are hot spots of GHG fluxes.

Soil GHG flux measurements were performed during the day (7.00 am – 5.00 pm) using a fast-box chamber technique (Hensen et al., 2013; Butterbach-Bahl et al., 2020). The CO_2 concentrations in the opaque chamber headspace were measured with an infrared gas analyzer (LI-840A & LI-850, LI-COR Biosciences, Lincoln, NE, USA), while CH_4 and N_2O concentrations were measured with an Off-Axis Integrated Cavity Output Spectroscopy (OA-ICOS) analyzer (Los Gatos Research, Inc., CA, USA). The GHG fluxes were calculated based on the linear changes of gas concentrations in the chamber headspace in the first 5-7 minutes following chamber closure. The CO_2 fluxes quantified using the opaque chambers represented either soil respiration (SR) (root and microbial respiration) or ecosystem respiration (ER) (root, microbial, and plant respiration). The CO_2 measurements in autumn across the entire landscape were SR since above-ground biomass was not included in the chambers during measurements. In contrast, the summer CO_2 measurements on arable and grasslands were ER since the above-ground vegetation was incorporated using chamber extensions, while the forest measurements remained as SR due to minimal above-ground vegetation on the forest floor. The day-to-day or diurnal variabilities related to our sampling strategy had a negligible effect on our data, with most of the variability in the data linked to spatial heterogeneities. Details of this finding as well as soil sampling, analysis, and flux measurement methods, are described in Wangari et al. (2022).

Table 1: List of the soil physico-chemical parameters and remotely-sensed data used in this study to upscale the GHG fluxes and details of the spatial resolutions of the maps.

		Resolution		
Category	**Predictor variables**	**Original**	**Final**	**Source**
Remotely-sensed data (RS)	Elevation	1 m	1 m	Hessische Verwaltung für Bodenmanagement und
	Slope	1 m	1 m	Calculated from elevation
	Aspect	1 m	1 m	
	Topographic wetness index (TWI)	1 m	1 m	
	Topographic position index (TPI)	1 m	1 m	
	Normalized difference vegetation index (NDVI)	10 m	1 m	Copernicus Sentinel-2 (European Space Agency)
	Green normalized difference vegetation index (GNDVI)	10 m	1 m	
	Normalized difference moisture index (NDMI)	20 m	1 m	
Soil physico-chemical parameters (SP)	Soil temperature (°C)	~ 25, 150, and 28 sites per km^2 in forest, grassland, and arable land	1 m	Interpolated from sampling point data measured in summer and autumn (Wangari et al. 2022)
	Gravimetric soil moisture (%)		1 m	
	pH		1 m	
	Bulk density ($g\ cm^{-3}$)		1 m	
	NO_3-N ($mg\ kg^{-1}$ dry soil)		1 m	
	NH_4-N ($mg\ kg^{-1}$ dry soil)		1 m	
	DOC ($mg\ kg^{-1}$ dry soil)		1 m	
	TDN ($mg\ kg^{-1}$ dry soil)		1 m	
	Soil TN (%)		1 m	
	Soil TOC (%)		1 m	
	CN		1 m	
	Sand content (%)		1 m	
	Silt content (%)		1 m	
	Clay content (%)		1 m	

2.2.2 Spatial interpolation of soil parameters

Upscaling soil GHG fluxes using the RF algorithm required spatial raster maps of the soil physico-chemical predictor parameters. Thus, we interpolated our measured point data to continuous landscape maps using the inverse distance weighted (IDW) approach in the System for Automated Geoscientific Analyses software (SAGA: QGIS) with a distance coefficient power of 1 (Gradka & Kwinta 2018). The spatial interpolations were performed per land use (forest, grassland, and arable land) and for each season (summer and autumn) due to significant variations in soil parameters such as soil moisture or inorganic N content across land uses and seasons (see Wangari et al., 2022).

2.3 Remote sensing data

We retrieved several landscape-scale remote-sensing images with spatial data representing potential drivers of soil GHG fluxes, such as vegetation cover and vegetation water content. Landscape elevation was acquired from a high-resolution (1 m) digital elevation model (DEM) retrieved from the Hessische Verwaltung für Bodenmanagement und Geoinformation on March 1, 2022 (link source). Slope and aspect were calculated from the

DEM using the “r.slope.aspect” function in QGIS. We further computed the topographic position index (TPI) and topographic wetness index (TWI) from the DEM using the terrain analysis plugin in QGIS. Vegetation information on chlorophyll and water content was derived from satellite bands of Sentinel-2 images. Satellite images with low (<1%) cloud cover were accessed from the ESA Copernicus Open Access Hub (link source; accessed on March 2021) using the Semi-Automatic Classification Plugin (Congedo, 2021) in QGIS for each field measuring period. The normalized difference vegetation index (NDVI) and the green normalized difference vegetation index (GNDVI) were calculated using the near-infrared (NIR), red, and green bands (Bannari et al., 1995; Gitelson and Merzlyak, 1998; Eq. 1 and 2). Compared to NDVI, GNDVI has a higher ability to detect differences in the chlorophyll content of plants, especially later in the vegetation period, due to the higher chlorophyll sensitivity of the green band in GNDVI than the red band in NDVI. The vegetation water content was estimated using the normalized difference moisture index (NDMI), which was computed using the NIR and short-wave infrared (SWIR) bands (Gao, 1996; Malakhov and Tsychuyeva, 2020; Eq. 3). We uniformly downscaled the resolutions of these remotely-sensed vegetation indices to match the 1 m spatial resolution of the DEM-derived data files (Table 1).

$$NDVI = \frac{NIR-RED}{NIR+RED} \quad \text{(Eq. 1)}$$

$$GNDVI = \frac{NIR-GREEN}{NIR+GREEN} \quad \text{(Eq. 2)}$$

$$NDMI = \frac{NIR-SWIR}{NIR+SWIR} \quad \text{(Eq. 3)}$$

2.4 Random Forest regression model

RF model development and prediction of the GHG fluxes were performed per land use (forest, grassland, and arable) because there were statistically significant differences observed in the measured fluxes and the underlying GHG flux controls of soil parameters for the different land uses (Wangari et al., 2022). For instance, N_2O fluxes and soil nitrate concentrations were up to two-fold higher in arable soils than in forestry or grassland soils. The CH_4 uptake rates of grassland and arable soils were lower than those of forest soils due to general differences in soil structure, nitrogen concentrations, and disturbances (Wangari et al., 2022). Modeling land use-specific GHG fluxes also enabled the identification of the best remotely-sensed predictors as the dominance of individual GHG production, consumption and processes may vary in dependence of land use. These best predictors can also be used as benchmark parameters in future studies that use a similar modeling framework to model GHG fluxes in single land-use landscapes. In contrast to land use, we trained models using merged summer and autumn point data to enable larger and temporally representative datasets for training models that could estimate low and high landscape GHG fluxes (Figure 2).

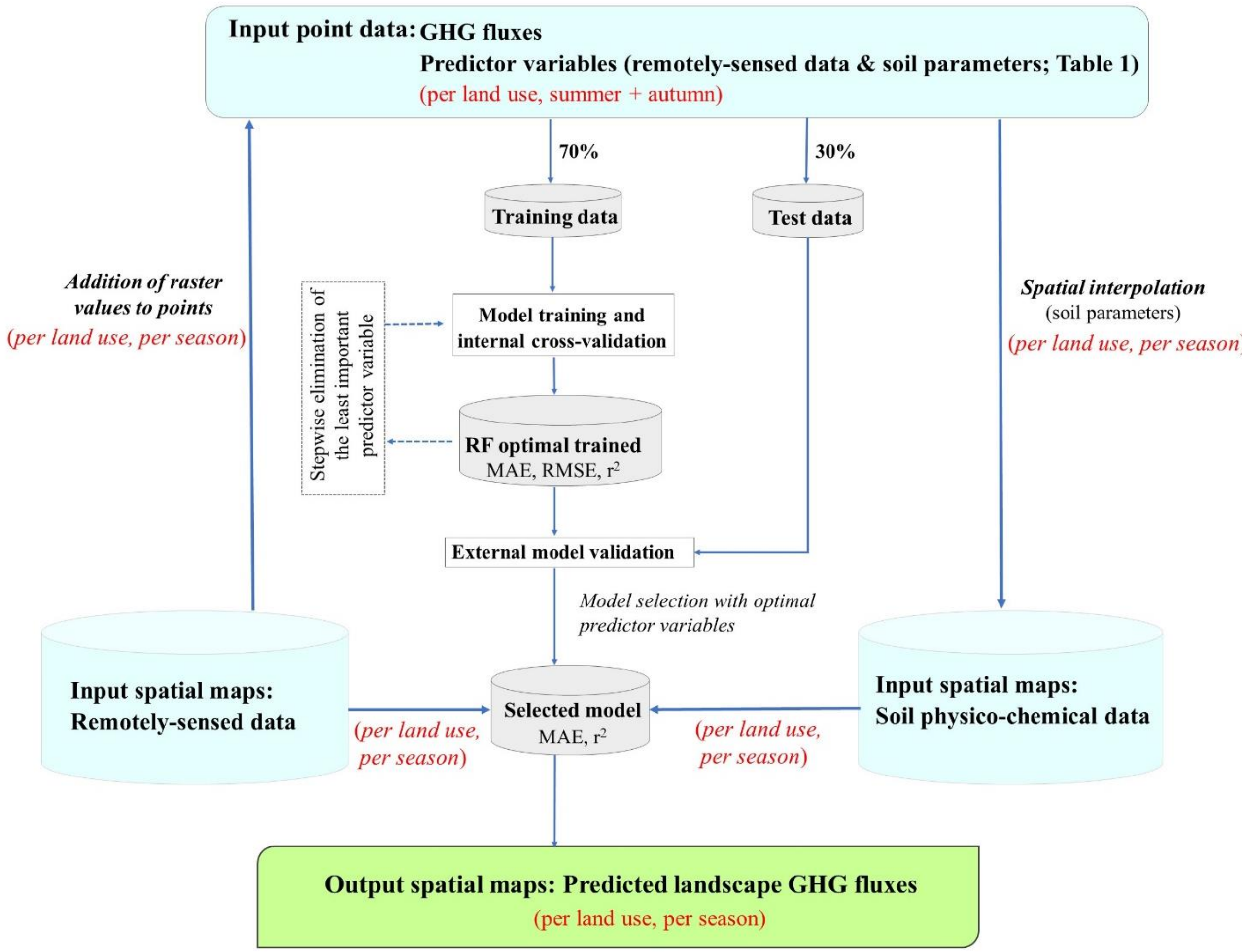

Figure 2: Workflow summary showing the input data (in blue), the approach used for RF model development and prediction of landscape fluxes, and the performance evaluation metrics (MAE, RMSE, and r^2).

We used the RF algorithm built in the CARET (classification and regression training) package in R to predict the soil GHG fluxes at a landscape scale (Breiman, 2001; Kuhn, 2008). For model development, the input datasets were split into a training and internal cross-validation set (70%) and an external test set (30%) using a stratified random sampling method. In addition to this hold-out approach of model validation, we defined a ten-fold (K=10) repeated cross-validation scheme on the 70% dataset using the 'trainControl' function to internally validate our trained models and prevent model overfitting (Berrar, 2018). This model validation strategy also minimized the limitation of the initial hold-out approach, providing a more spatially robust model validation step (Meyer and Pebesma, 2022). A seed value of 123 was specified using the 'set.seed' function to enable reproducible results each time we ran a specific model. The random forest's most important hyperparameters (mtry = number of variables at each tree, and n.tree = the number of trees) were tuned automatically within the CARET package. Tuning was done automatically after a sensitivity analysis (based on assessing the mean absolute error: MAE) was performed 10 times to choose the best mtry and n.tree, resulting in the optimal trained model, i.e., the one with the lowest MAE. The predictor variables in the optimal trained model were then ranked according to their importance using the RF variable importance measure in the 'varImp' function. Subsequently, stepwise elimination of the least essential variable was performed to quantify the predictive power of landscape GHG fluxes using fewer predictor variables (Figure 2).

To assess the effectiveness of various types of predictors in modeling landscape fluxes, we defined three categories of datasets, namely remote-sensing (RS), site-measured soil physico-chemical parameters (SP), and combined data (CD) (Table 1). Several RF models were trained following the stepwise elimination of the least important variables in each data category (RS, SP, CD). Since 88% of CH_4 fluxes were negative and 86% of N_2O fluxes were positive (Wangari et al., 2022), we additionally trained models using only the negative CH_4 and positive N_2O flux datasets to compare their performances with the models built with all (positive and negative) fluxes.

2.5 Model performance assessment and prediction of landscape fluxes

The performance assessment metrics of the trained models included MAE, root mean square error (RMSE), and the coefficient of determination (r^2) from the internal cross-validation. The final models for predicting landscape fluxes in each data category (RS, SP, CD) were selected based on the highest possible r^2 with a relatively low MAE. For each season and land use, the surface maps of the respective predictor variables in the final models were merged using the raster brick function in R. The spatial fluxes for each land use were then predicted based on the selected model and the input raster brick using the 'predict' function in R. To improve the prediction performance, the non-normal distributed (SR/ER_CO_2 and N_2O) fluxes were log-transformed before model development. After prediction, the transformed fluxes were retransformed using an exponential function.

Further evaluation of the model performances was conducted through linear regression and correlation analysis of observed against retransformed predicted fluxes for all sampling sites. An additional external validation step was performed using the measured and predicted fluxes of the sampling sites in the 30% test dataset that was excluded from the model development. For this analysis, we compared the predicted mean fluxes (using RS, SP, and CD datasets) with the observed mean fluxes. Analyses of variances (Type II) from linear mixed-effects models ("nlme" package in R) were used to compare these arithmetic means. The fixed effects in the mixed models were seasons (summer and autumn) and GHG flux type (measured and predicted fluxes from the RS, SP, and CD datasets). Random effects of site variability were also included in the mixed models. The measured and predicted fluxes were log-transformed to the normality assumption. A Tukey post-hoc test (p-value <0.05) of least square means was used on the mixed models to identify statistically significant differences between the measured, RS-predicted, SP-predicted, and CD-predicted fluxes.

Since many traditional GHG upscaling approaches rely on aggregated fluxes (area-weighted averages), we also estimated spatial fluxes for the summer and autumn seasons using this technique. GHG fluxes were aggregated on the landscape scale by multiplying the average fluxes measured for each land use by the area of each land use. We compared the total landscape fluxes upscaled using this conventional aggregation technique of average fluxes with the spatial fluxes predicted using the modeling approach.

2.6 Identification of summer and autumn GHG ‘hot’ and ‘cold’ spots from predicted landscape fluxes

Statistical approaches were deployed to identify areas that may have disproportionately contributed to the overall landscape GHG fluxes (e.g., van Kessel et al., 1993; Mason et al., 2017). We defined the threshold for hot spots using the sum of the median (M) flux and the interquartile (Q3-Q1) flux range (Eq. 4). Thus, the hot spots within the landscape were identified as the areas with flux values greater (lower for CH_4 uptake) than the set hot spot threshold. We fixed an inverse threshold (Eq. 5) for cold spots and identified cold spot patches with fluxes below (above for CH_4 uptake) this threshold. Common emission hot spots were defined as the areas with overlapping elevated emissions of the three GHG fluxes (SR/ER-CO_2, CH_4, and N_2O) within the landscape. The average (summer and autumn) landscape fluxes were used to identify the hot and cold spots. We also calculated season-specific thresholds to compare the increase and decrease of hot and cold spot areas between summer and autumn.

$$Hot\ spot\ threshold = M + (Q3 - Q1) \qquad \text{(Eq. 4)}$$

$$Cold\ spot\ threshold = M - (Q3 - Q1) \qquad \text{(Eq. 5)}$$

3. Results

3.1 RF model performance

The performance of the final models selected for the prediction of landscape fluxes varied across input datasets (RS, SP, and CD), GHG fluxes (SR/ER_CO_2, CH_4, and N_2O), and land use (forest, grassland, and arable land) (Table 2). The predictive performance (r^2) from the internal cross-validation step was higher in the models using the CD dataset (range: 0.15 – 0.78) than those using the RS (range: 0.13 – 0.73) and SP (range: 0.15 – 0.63) datasets (Table 2). The RF models predicting SR/ER_CO_2 fluxes had much higher r^2 (range: 0.45 – 0.78) than those predicting N_2O and CH_4 fluxes (range: 0.13 – 0.56). Arable ecosystem models resulted in much better predictions of SR/ER_CO_2 (r^2 range: 0.63 – 0.78) and N_2O (r^2 range: 0.45 – 0.56) fluxes compared to those for forest and grassland ecosystems across all data categories (Table 2). The prediction of CH_4 fluxes was also better for arable lands, but only when using the RS data (Table 2). Stepwise elimination of the least important variables had a minimal effect on the performances of the trained models (Table B1-B5 in Appendices). The selected models for the different categories of datasets (RS, SP, and CD) had varying predictor variables across land uses. The forest and grassland models required the most (5 and 6) predictor variables. In contrast, the least number of predictors (2) were mainly observed for models describing GHG fluxes from arable soils, especially in the RS and SP categories (Table 2).

Comparing the models (CD) applied to predict the landscape fluxes, the site-measured soil moisture content was a key predictor variable for all three GHG fluxes across land uses. In addition to soil moisture, the measured soil nitrogen content (NH_4 or SN) and remotely sensed vegetation indices (NDVI, GNDVI, or NDMI) were prevalent predictors of landscape SR/ER_CO_2 fluxes. Soil nitrogen content (NO_3 or CN) was also a recurrent predictor of CH_4 fluxes across land uses. However, the landscape CH_4 models had other varying predictors, such as aspect and soil temperature in forest models, pH and clay in grassland, and vegetation indices in arable ecosystem models. For N_2O, soil inorganic nitrogen (NH_4 or NO_3) concentrations predicted the fluxes in the forested areas, while vegetation indices were common predictors in grassland and arable ecosystems (Table 2).

Further assessment of model performance was performed through an external validation step comparing the mean of observed and predicted fluxes in the test dataset (n=∼140 per flux). The mean measured CO_2 and CH_4 fluxes were similar to the predicted carbon fluxes across all the data categories (RS, SP, CD) within each season. In contrast to the carbon fluxes, the measured N_2O fluxes were significantly lower than the predicted fluxes in autumn (Figure A1 in Appendices).

Table 2: List of predictor variables and the performance of the selected RF models using either remote sensing (RS), soil physico-chemical parameters (SP), or combined (remote sensing and soil parameters) data. The model selection was made after a cross-validation (10-fold) step whereby the model's predictive power was tested based on unseen data to avoid overfitting.

				10-fold cross validation		
Flux type	**Land use**	**Category**	**Predictor variables**	**R^2**	**RMSE**	**MAE**
SR/ER-CO_2-C (mg m^{-2} h^{-1})	Forest (SR)	Remotely-sensed data (RS)	NDVI, GNDVI, NDMI	0.45	1.76	1.55
	Grassland (ER)		NDVI, GNDVI, NDMI	0.46	1.88	1.61
	Arable (ER)		Elevation, NDVI, GNDVI, NDMI	0.73	1.76	1.58
CH_4-C (μg m^{-2} h^{-1})	Forest		Aspect, NDVI, GNDVI	0.14	46.38	36.15
	Grassland		Elevation, TPI, NDVI, NDMI	0.15	29.23	21.53
	Arable		GNDVI, NDMI	0.35	50.79	34.72
N_2O-N (μg m^{-2} h^{-1})	Forest		NDVI, GNDVI, NDMI	0.13	18.46	18.62
	Grassland		NDVI, GNDVI, NDMI	0.13	17.87	18.26
	Arable		GNDVI, NDMI	0.53	18.32	18.50
SR/ER-CO_2-C (mg m^{-2} h^{-1})	Forest (SR)	Soil physico-chemical parameters (SP)	Soil moisture, pH, NH_4-N, DOC	0.49	1.72	1.53
	Grassland (ER)		Soil moisture, NH_4-N, TDN	0.54	1.79	1.55
	Arable (ER)		Soil moisture, SN	0.63	1.94	1.70
CH_4-C (μg m^{-2} h^{-1})	Forest		Soil temperature, soil moisture, pH, NO_3-N, silt	0.16	44.29	33.87
	Grassland		Soil moisture, pH, NO_3-N, DOC, CN, clay	0.29	25.59	18.62
	Arable		DOC, CN	0.29	44.51	32.65
N_2O-N (μg m^{-2} h^{-1})	Forest		Soil moisture, NO_3-N, NH_4-N	0.15	18.49	18.65
	Grassland		Soil moisture, NH_4-N, CN, clay	0.22	18.02	18.37
	Arable		Soil moisture, NO_3-N, SN, CN	0.46	18.28	18.48
SR/ER-CO_2-C (mg m^{-2} h^{-1})	Forest (SR)	Combined data (CD)	NDVI, GNDVI, NDMI, soil moisture, NH_4-N, DOC	0.57	1.64	1.48
	Grassland (ER)		GNDVI, soil moisture, NH_4-N	0.57	1.76	1.54
	Arable (ER)		NDVI, GNDVI, soil moisture, SN	0.78	1.68	1.51
CH_4-C (μg m^{-2} h^{-1})	Forest		Aspect, soil temperature, soil moisture, NO_3-N	0.21	43.50	34.58
	Grassland		Soil moisture, pH, NO_3-N, CN, clay	0.30	25.38	18.29
	Arable		GNDVI, NDMI, CN	0.31	47.59	33.30
N_2O-N (μg m^{-2} h^{-1})	Forest		Soil moisture, NO_3-N, NH_4-N	0.15	18.49	18.65
	Grassland		NDVI, soil moisture	0.25	18.05	18.37
	Arable		NDVI, GNDVI, NDMI, soil moisture	0.56	18.36	18.52

3.2 Observed versus predicted GHG fluxes

The measured and predicted GHG fluxes for all the sampling points had significant ($p<0.001$) linear relationships (Figure 3). The model predictions of SR/ER_CO_2 fluxes were better (r^2; 0.49 – 0.67) than for soil CH_4 (r^2; 0.39 – 0.46) or N_2O (r^2; 0.34 – 0.43) flux predictions across the three input datasets. Based on the estimated slopes, the predicted values were 35 – 46% lower than the measured values for SR/ER_CO_2 fluxes. Compared to CO_2, the CH_4 and N_2O predicted fluxes were lower (CH_4 53 – 58%; N_2O 60 – 65%) than the measured fluxes, primarily due to the underestimation of high fluxes. Based on r^2 values, the performances of the different predictor datasets were in the order of CD>RS>SP for carbon fluxes and CD>SP>RS for N_2O fluxes (Figure 3).

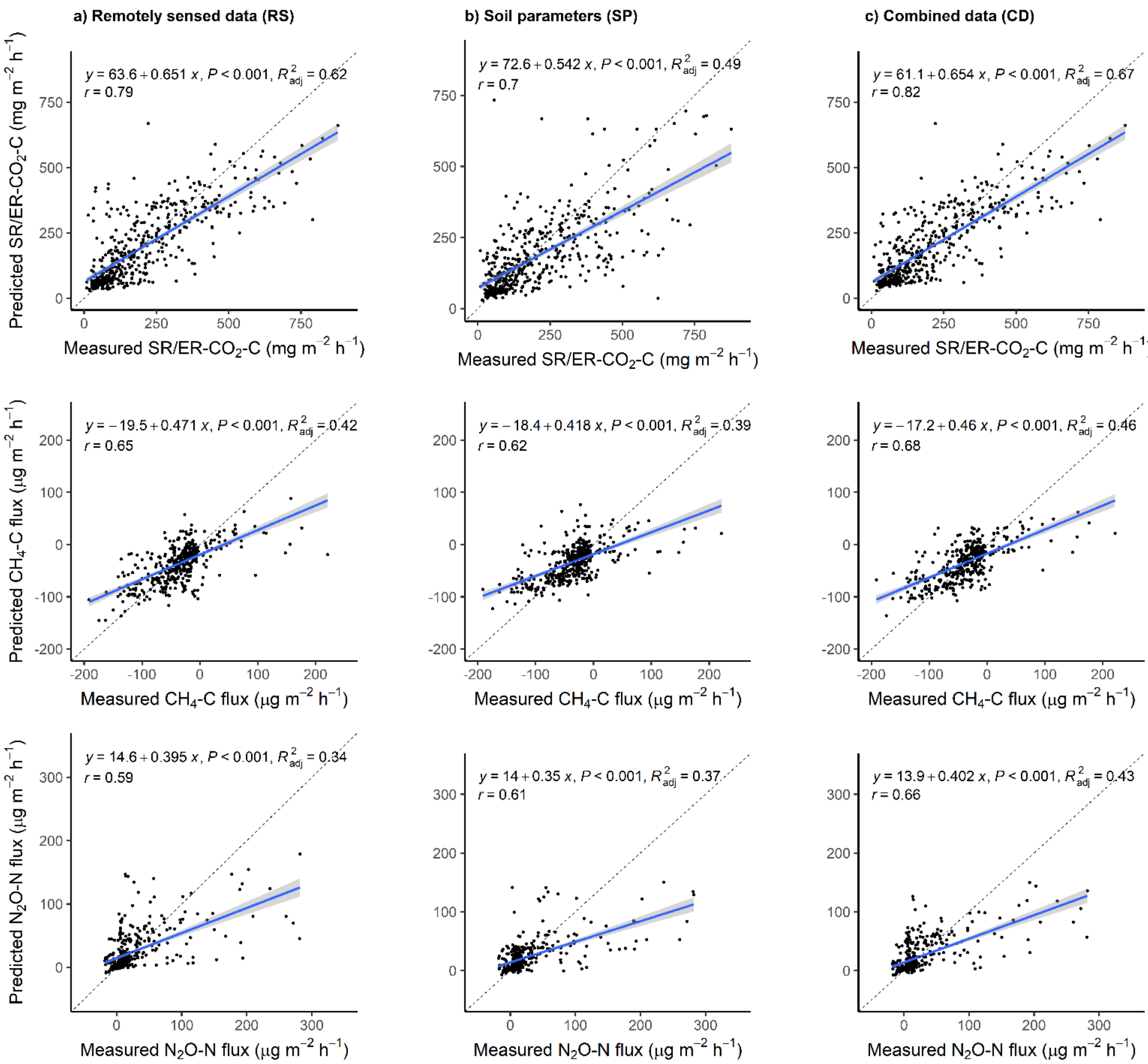

Figure 3: Linear regressions (with 95% confidence bands) of the measured and predicted GHG fluxes using remotely sensed data (RS), soil physico-chemical parameters (SP), and combined data (CD). GHG fluxes from all the sampling locations (both the 70% training data and the 30% test data) were considered in this regression analysis. The dotted line represents the 1:1 line.

3.3 Spatio-temporal variation in modeled landscape-scale fluxes

Predicted landscape fluxes for the summer and autumn seasons ranged from +27.7 – +733.3 mg m^{-2} h^{-1} for CO_2-C, -148.4 – +89.4 µg m^{-2} h^{-1} for CH_4-C, and from -8.8 – +189.9 µg m^{-2} h^{-1} for N_2O, and did not differ much in dependence of the input dataset used (RS, SP, or CD) (Table B6 in Appendices). However, the predicted flux ranges for the landscape were narrower than the measured fluxes, which ranged from 8.7 to 877.0 mg m^{-2} h^{-1} for CO_2-C, from -214.1 – +221.2 µg m^{-2} h^{-1} for CH_4-C and from -18.1 – +281.8 µg m^{-2} h^{-1} for N_2O-N. Since the CD dataset revealed models with better predictions for all GHG fluxes than the RS and SP datasets, we used GHG fluxes predicted from CD predictors for seasonal and land use comparisons.

Most of the landscape area (99.2%) had higher SR/ER_CO_2 fluxes in summer than in autumn, with a small proportion of arable and grassland ecosystems having an opposite trend. Around 76% of the landscape also had higher N_2O fluxes in summer than in autumn. Approximately 24% of the landscape, primarily in the forested areas, had higher N_2O fluxes in autumn than in summer. CH_4 uptake rates were lower in summer than in autumn in most of the landscape (63%), especially in arable and grassland soils. However, an opposite trend was found for about 37% of the landscape area, dominated by forests, where CH_4 uptake rates were lower in autumn than in summer (Figure 4c).

High spatial heterogeneities (within short distances of <2 m) of the predicted landscape fluxes were observed in each land use. Overall, spatial variations were more prominent in summer than in autumn (Figure 4; Table B6 in Appendices). The spatial variability of SR/ER_CO_2 fluxes was higher (with a range of up to 2.6-folds) on arable soils than forest and grassland soils, with multiple patches of low fluxes surrounded by high fluxes. CH_4 fluxes on arable lands were also heterogeneous, with the soils acting as CH_4 sinks and sources within a few meters, especially during summer (Figure 4a). For N_2O fluxes, high spatial heterogeneities were observed on grassland soils in summer, as N_2O uptake and emission of the same or even higher order of magnitude occurred at neighboring pixels. Arable soils in autumn were also highly heterogeneous, with patches of high N_2O fluxes surrounded by low fluxes (Figure 4b).

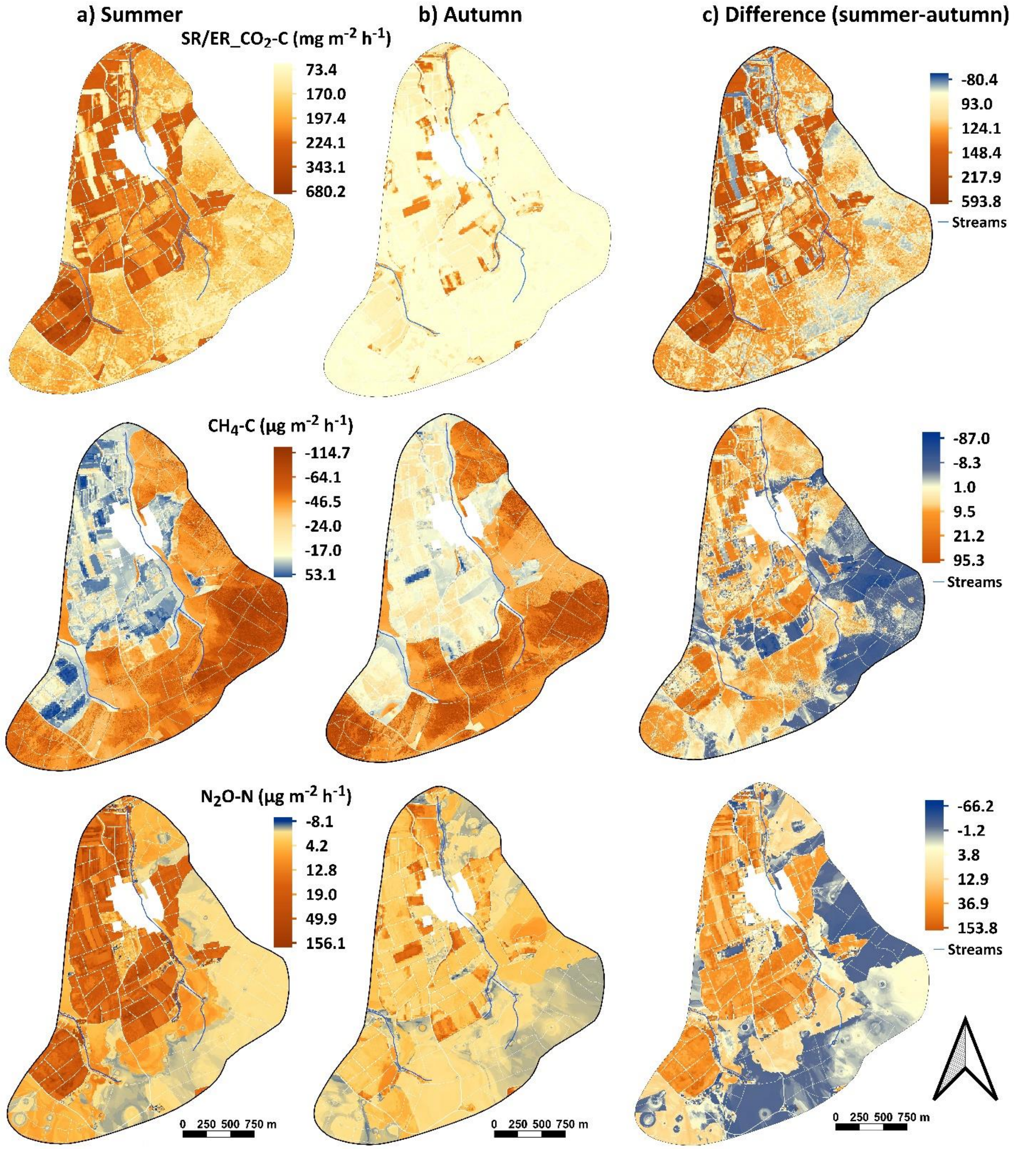

Figure 4: Landscape maps of SR/ER_CO_2, CH_4, and N_2O for (a) summer, (b) autumn seasons, and (c) the difference maps showing the variation of the autumn from the summer fluxes. The surface fluxes were predicted using RF models trained with combined (remote-sensing and site-measured soil parameters) data (CD; Table 2).

3.4 Summer and autumn hot spots and cold spots

The hot and cold spots of the GHG fluxes were identified from the average (summer and autumn) upscaled landscape fluxes (Figure 5a). Using equation 4, the SR/ER_CO_2 and N_2O spatial hot spots had threshold values >231.5 mg CO_2-C m^{-2} h^{-1} for CO_2 and >36.8 µg N_2O-N m^{-2} h^{-1} for N_2O. These hot spots covered a relatively small portion (~16.7%) of the landscape, yet they played a significant role, especially the N_2O hot spots, which accounted for 42% of the landscape fluxes. Around 29% of the total SR/ER_CO_2 landscape flux emanated from the hot spot areas (Figure 5). Overall, the SR/ER_CO_2 and N_2O hot spots were mainly located on arable lands (77.0% and 94.5%, respectively) and grasslands (22.9% and 5.5%, respectively). Compared to the SR/ER_CO_2 and N_2O hot spots, the hot and cold spots of CH_4 uptake were observed in smaller regions (3.1% and 7.3%) of the landscape with high soil CH_4 uptake rates (>87.3 µg CH_4-C m^{-2} h^{-1}) and low soil CH_4 uptake rates (<3.4 µg CH_4-C m^{-2} h^{-1}). The CH_4 uptake hot spots, exclusively on the forested soils, offset 8% of the landscape CH_4 fluxes (Figure 5). The cold spots occupied 7% of the landscape and were primarily on arable soils (99.6%), accounting for 2% of the landscape's CH_4 emissions.

Common hot spots, with overlapping areas with elevated GHG emissions (i.e., SR/ER_CO_2 and N_2O hot spot areas and CH_4 uptake cold spot areas), were mainly on arable soils (99.87%), with few located in grasslands (0.12%) and forests (0.01%). Overall, these patches covered 1.5% of the landscape area and contributed 5%, 1%, and 8% of the SR/ER_CO_2, CH_4, and N_2O emissions within the landscape (Figure A2 in Appendices). Based on field observations of the sampling sites (n=14) in the common hot spots, the sites at arable lands were either cropped with barley or wheat. These arable common hot spots also had higher soil moisture content and NO_3 concentrations than the average values recorded at all the other sampling locations. The common hot spots in the forest were found along the riparian zones if either nitrogen-fixing alder trees were present or if grazed by cattle. Soil moisture (%), DOC, NO_3, and NH_4 concentrations at these sites were also higher than mean values across all sampling points. The grassland common hot spot regions were densely covered by nitrogen-fixing clover, with some located along the riparian zones (Figure A3; Table B7 in Appendices).

Comparison of the GHG emission hot spots in summer and autumn using season-specific thresholds revealed significant shifts in their geo-locations between the two seasons (Figure A4 in Appendices). SR/ER_CO_2 hot spot regions expanded by 46% from summer to autumn, even though the emissions from the former season were higher. Unlike CO_2, N_2O emission hot spots and CH_4 uptake cold spots contracted by 23% and 86%, respectively, from summer to autumn.

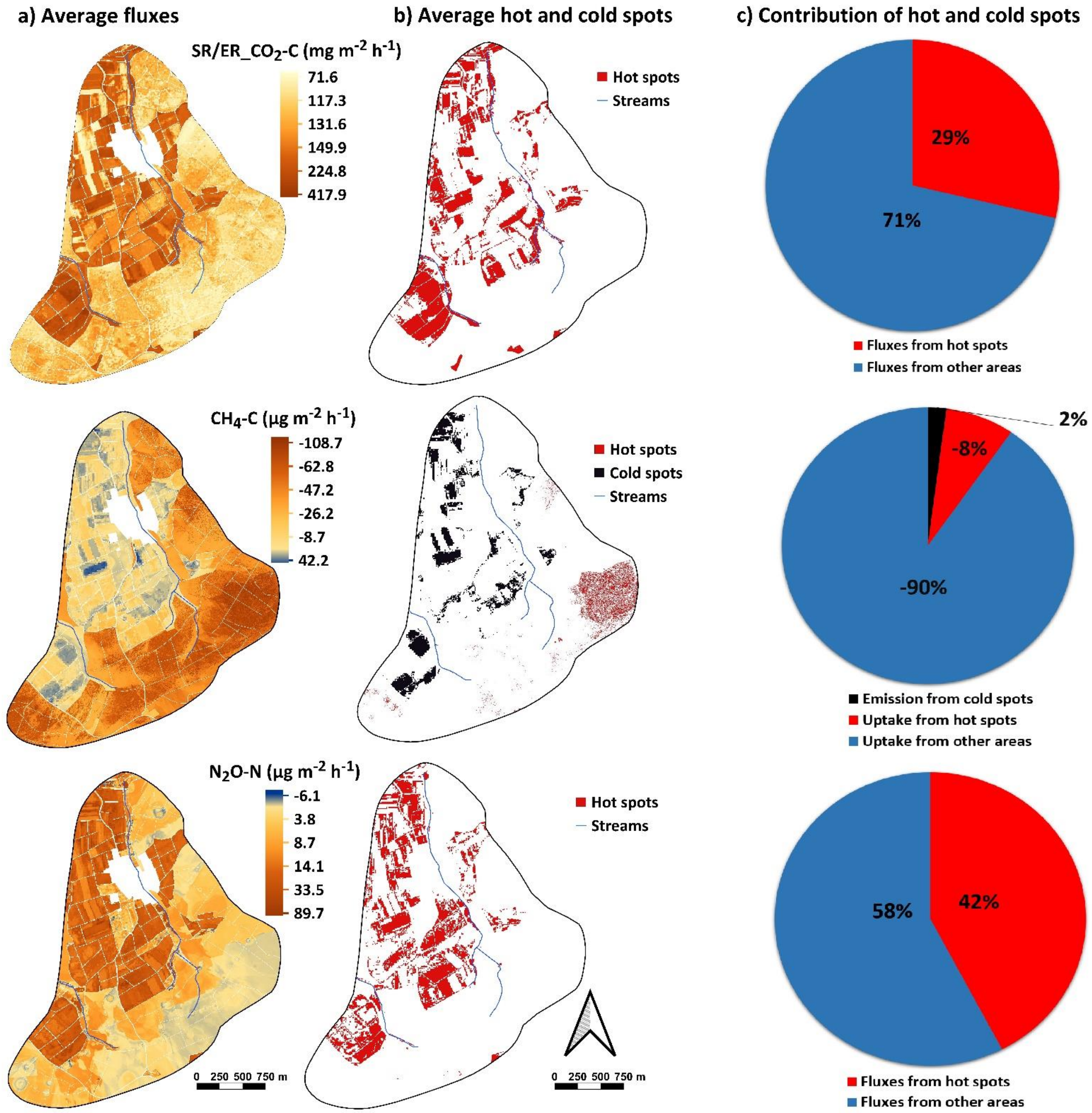

Figure 5: Maps showing (a) the average GHG fluxes and (b) the average hot spot and cold spot regions on the landscape for the summer and autumn seasons. The pie charts show the contribution (%) of hot and cold spots to total landscape fluxes. For this analysis, landscape fluxes were predicted using the combined data (CD; Table 2; Figure 3).

3.5 Comparison of upscaling approaches

Seasonal differences in spatial patterns and magnitudes of GHG fluxes were observed for upscaled fluxes using either RF modeling or mean values of measured fluxes. In both approaches, the SR/ER_CO_2 and N_2O landscape fluxes were an order of magnitude higher in summer than in autumn. The CH_4 uptake rates were higher in autumn than in summer but within the same order of magnitude. In summer, the landscape-scale SR/ER_CO_2 and N_2O fluxes estimated using the area-weighted average approach were 26% and 50% higher than the RF-modelled fluxes. The contrary was observed in autumn, where the later methodology produced slightly (4% and 11%) higher fluxes than the area-weighted mean estimates.

The entire landscape CH_4 uptake estimates for autumn using the area-weighted mean were 16% higher than the modeled estimates. Contrary to autumn, the area-weighted mean approach had slightly lower estimates of CH_4 uptake than the modeling approach in summer. Additionally, the CH_4 surface flux estimates for the whole arable land in summer were net sinks (-0.9 CH_4-C g h^{-1}) using the RF modeling approach contrary to the net sources (15.5 CH_4-C g h^{-1}) estimated by the area-weighted mean method. Overall, the total landscape fluxes estimated using the area-weighted mean approach had up to two orders of magnitude higher uncertainty (standard error) than the modeled landscape fluxes (Figure 6).

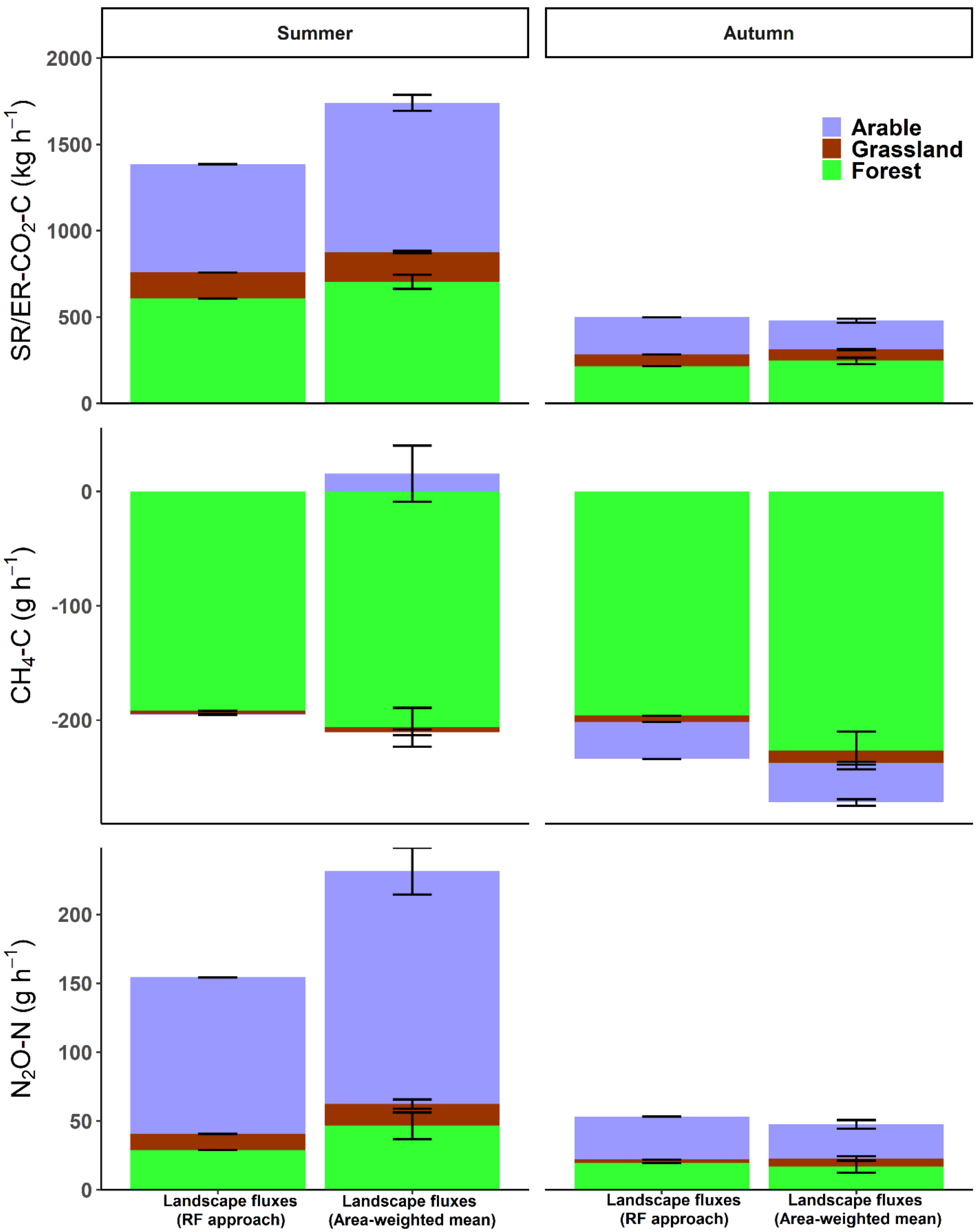

Figure 6: The total landscape fluxes (+SE) predicted using random forest (RF) models (with combined dataset) and the fluxes estimated using the area-weighted mean approach where the average point-measured fluxes were multiplied by the landscape area.

4. Discussion

4.1 Efficiency of in-situ soil parameters and remote-sensing data in upscaling GHG fluxes

Our study showed that remotely-sensed (RS) data and measured soil parameters (SP) could effectively upscale soil-atmosphere CO_2, N_2O, and CH_4 fluxes from point chamber measurements across a heterogeneous landscape with mixed land uses. This approach represents a Tier 3 approach of upscaling landscape GHG fluxes, as it provides spatially explicit GHG fluxes at a high resolution comparable to modeled fluxes using either process-based models or statistical functions (e.g., Haas et al., 2013; Tiemeyer et al., 2020; Koch et al., 2023). The improved prediction performance of the combined data (CD) sources indicates the importance of incorporating controls of soil GHG fluxes that are remotely sensed and ground-based field observations. The prediction models in this study suggested that the Sentinel-2-derived indices (NDVI, GNDVI, and NDMI) were more effective predictors than the DEM-derived terrain attributes (elevation, slope, aspect, TWI, and TPI). This finding is supported by the appearance of the Sentinel-2-derived indices in the prediction models of the three GHGs, contrary to only one DEM index (aspect) that appeared in the CH_4 flux prediction models for the forest ecosystem. The minor role of DEM indices in this study can be attributed to the relatively flat terrain of our study landscape (Figure 1b) and is further backed by the lack of spatial variation in the measured GHG fluxes with slope, yet slope was considered during site stratification (Wangari et al., 2022). Another possible explanation could be that soil wetness, a common predictor of all the GHG fluxes across the landscape, was better represented by the site-measured soil moisture content and the NDMI index (vegetation water content), than any of the DEM terrain attributes, including the TWI that focuses on moisture conditions, as they lack a temporal dimension.

Compared with other studies that have upscaled GHG fluxes using the random forest algorithm, we considered more site-measured data on soil parameters, all three GHG fluxes, and different land uses (Table 3). Moreover, point selections for measurements were done by implementing a stratified sampling plan that represented the spatial variability of several landscape characteristics, specifically land use, soil type, and slope (Wangari et al., 2022). The prediction accuracies of soil respiration for our mixed forest ecosystem (3.3 km^2) were slightly better than those reported for a smaller forested headwater watershed (0.12 km^2) in Maryland, USA (Warner et al., 2019). Our CH_4 prediction performance for forest soils was comparable to those of a boreal forest landscape (Vainio et al., 2021). However, our CH_4 prediction performance was up to 3.6-fold lower than those of a forested headwater watershed and peatland soils, which can be attributed to higher and more homogenous CH_4 production in such ecosystems (Warner et al., 2019; Räsänen et al., 2021). Our CH_4 and N_2O model prediction accuracies for arable soils were better than those for arable soils in New South Wales, Australia, which only considered input data from ground-based sensors such as soil pH and clay content (McDaniel et al., 2017). Nevertheless, caution has to be taken when interpreting any conclusions from these study comparisons due to the limitations of different model validation techniques, different predictor variables used for modeling, and the different ecosystems and spatial scales of measurement and predictions.

4.2 Seasonal variability of landscape fluxes

The GHG fluxes predicted by the RF model in this study revealed seasonal trends of up to 3-fold higher CO_2 and N_2O fluxes in summer and 1.2-fold higher CH_4 uptake in autumn, which were also evident in the measured fluxes at the sampling points (Wangari et al., 2022). These trends can be attributed to seasonal changes in soil parameters and vegetation within the landscape that were well captured by the measured soil parameters and Sentinel-2-derived indices in the prediction models. The higher soil moisture, mineral nitrogen, and vegetation cover observed during the summer growing season enhanced the respiration rates (SR/ER_CO_2) and N_2O emissions, particularly in arable ecosystems, which were flux hot spots for both gases. Root respiration of growing plants can also enhance N_2O production through denitrification by creating anaerobic conditions and supplying labile exudates to denitrifying microbes (Butterbach-Bahl & Dannenmann, 2011; Malique et al., 2019). Previous studies have shown that higher mineral nitrogen and soil moisture content can enhance N_2O production in soils through an increased supply of substrates and the creation of anaerobic conditions that enhance denitrification rates (Barton et al., 1999; Ciarlo et al., 2007; Butterbach-Bahl et al., 2013). The lower CH_4 uptake rates in summer can be primarily explained by the observed higher soil moisture content, which has been previously reported to hinder CH_4 oxidation by slowing down gas (atmospheric CH_4) diffusion in soils (Le Mer & Roger, 2001).

The high-resolution (1 m pixel size) scaled-up fluxes could also identify detailed temporal patterns of the GHG fluxes across the landscape, thus revealing trends that were otherwise undetectable in the aggregated measured (point) fluxes. To illustrate, parts of the landscape (24% and 37%) showed even opposite trends of higher N_2O fluxes and lower CH_4 uptake rates in autumn, and these areas were predominantly in the mixed forest ecosystem. Such fine-scale patterns of GHG fluxes result from land use-specific local effects depending on the season. For example, decaying fallen leaves during autumn can favor denitrification in forest soils by increasing carbon and mineral N availability (e.g., Groffman & Tiedje, 1989), which may not be true for grassland or arable ecosystems due to harvesting and mowing. The higher CH_4 uptake rates in summer could be due to warmer summer temperatures leading to drier, more aerated forest soils that promote CH_4 oxidation (Steinkamp et al., 2000). This finding is supported by the importance of aspect as a predictor of landscape CH_4 fluxes in the forest ecosystem, which influences the amount of incoming radiation an area receives.

4.3 Importance of hot spots and cold spots of landscape-scale GHG fluxes

The high spatial resolution of our predicted GHG fluxes enabled the identification of areas across the landscape that functioned as hot spots (of soil CH_4 uptake, SR/ER_CO_2, and N_2O) or cold spots of soil CH_4 uptake. Based on field observations and analyses of important predictor variables, the existence of these hot and cold spots was primarily driven by human activities such as fertilizer application, crop growing and tillage, and landscape environmental parameters related to seasonality and proximity to riparian areas. This finding is supported by the primary association of the SR/ER_CO_2 and N_2O hot spots and CH_4 uptake cold spots within arable ecosystems since these systems showed higher soil mineral nitrogen concentrations than grassland and forest soils. The hot spots of SR/ER_CO_2 and N_2O observed on the grassland ecosystem can be attributed to the primary location of grasslands along the riparian areas. Increased soil moisture values and higher soil C contents, key characteristics of the riparian regions, have also been reported to drive elevated soil GHG fluxes (Kaiser et al., 2018; Vainio et al., 2021).

Spatial hot spots of SR/ER_CO_2 and N_2O played a crucial role in determining total landscape fluxes, accounting for up to 42% of the total predicted landscape fluxes despite their relatively low (~16%) coverage area. Such high contributions suggest that failure to capture these hot spots results in large uncertainties in landscape GHG flux estimates. Overall, the contribution of the hot spot areas (of CO_2, N_2O, and CH_4 emissions) to the landscape fluxes decreased in the order of $N_2O>CO_2>CH_4$. This finding emphasizes the importance of increasing the spatial coverage of N_2O measurements to include more hot spot areas, as they can introduce enormous uncertainty in landscape fluxes if not quantified. A similar finding emphasizing the importance of N_2O flux heterogeneities has been concluded in a previous study, which recorded more sampling locations required for improved N_2O flux estimates than CO_2 and CH_4 at a landscape scale (Wangari et al., 2022).

Identifying common patches with elevated emissions of all three GHGs can inform priority areas for implementing localized mitigation measures within a landscape. These common patches covered only 1.5% of our landscape (~0.2 km^2) and had the highest GHG fluxes contributing around 5%, 1%, and 8% of the landscape CO_2, CH_4, and N_2O emissions. The location of these patches primarily (99.9%) on arable land emphasized the significant role of focusing on mitigating GHG fluxes from arable soils. Because most of the common GHG hot spots in the arable soils were also in areas with high water content, mitigation strategies that aim to adjust the fertilizer application rates at specific areas holding more water may successfully lower the emissions (e.g., Hassan et al., 2022). In contrast to hot spot regions of elevated GHG emissions, CH_4 uptake hot spots inform future mechanisms for leveraging the GHG sink ability of soils, such as expanding local forests. This finding is supported by uptake hot spots identified on forest soils in this study, offsetting 8% of the total landscape CH_4 flux. The expansion of forested areas will also likely have a high mitigation impact via CO_2 sequestration. Although some of the above strategies are currently applied at broader scales (1 km^2), localized mitigation strategies may be required at smaller scales (<100 m^2), especially at highly heterogeneous landscapes with a high variability of agricultural practices. We also found significant shifts in the geo-locations of hotspot regions between summer and autumn, suggesting that seasonal effects of land management (e.g., fertilization, harvesting, and residue management) and soil conditions may also lead to a temporal expansion or contraction of the hot spot regions. This finding further emphasizes the need for time-based mitigation strategies, such as considering fertilizer application times, which not only target the spatial hot spots but also consider the temporal patterns that result in peak emissions (e.g., Wagner-Riddle et al., 2020).

4.4 Comparison of upscaling approaches

Contrary to the area-weighted upscaling approach of spatial aggregation of chamber fluxes (Webster et al., 2008; Molodovskaya et al., 2011; Rosenstock et al., 2016), random forest modeling allowed us to estimate the entire spatial distributions of the fluxes at high spatial resolution (1 m pixel size), capturing both cold spots and hot spots. In agreement with our hypotheses, the landscape fluxes were either over or under-estimated by the area-weighted average approach compared to the RF modeling approach. The overestimated landscape CO_2 and N_2O fluxes by the area-weighted average approach of up to 50% during the peak summer season suggest an overrepresentation of the high fluxes measured at most of the sampling points, resulting in elevated mean and upscaled fluxes. Furthermore, landscape CH_4 uptake rates were overestimated by the area-weighted average approach during the peak autumn season. Previous studies have also observed a similar trend of elevated mean CH_4 uptake rates at measured sites, which they attributed to the over-representation of high uptake rates during the peak uptake seasons (Warner et al., 2019). Conversely, the underestimation of CO_2, N_2O, and CH_4 uptake by the area-weighted average approach, especially on arable soils, coincided with the low flux season, implying reduced mean fluxes due to the overrepresentation of the low fluxes. An alternative explanation of the differences in landscape flux estimates from both approaches could be the underestimation of high fluxes by the RF models, which we also found in our study. However, the landscape means of RF predicted and measured fluxes from 30% of our sampled sites were primarily similar (Figure A1 in Appendices), suggesting that the lack of spatial representation of all hot and cold spots by the area-weighted mean approach rather than the inability of the RF models to reproduce high values accounted for the findings above.

Collectively, our results illustrated that the representativeness of landscape fluxes using aggregated chamber fluxes might be influenced by the spatial and temporal heterogeneity of the fluxes. This finding aligns with previous results on the required number of chamber measurement locations for reliable landscape fluxes that varied with land use and season (Warner et al., 2019; Wangari et al., 2022). The high (50%) overestimation of landscape N_2O fluxes suggested the higher sensitivity of reliably estimating N_2O fluxes using the (aggregated means) conventional method. Previous studies have also emphasized the importance of N_2O fluxes in constraining uncertainties in landscape flux quantification (e.g., Wangari et al., 2022). Compared to the suggested way of lowering landscape-scale flux uncertainties in the conventional estimates by increasing the number of chamber measurements within a landscape (Wangari et al., 2022), the modeling approach can be a less resource-intensive alternative.

Combining high-resolution remote sensing data and measured soil parameters to upscale the chamber fluxes reduced the biases and the aforementioned landscape-scale flux uncertainties. The reduced uncertainties in the modeled landscape fluxes can be attributed to the relation of multiple underlying controls of soil GHG fluxes, which have high seasonal and spatial variability. Remote sensing datasets have unlimited spatial extents with high spatial resolution and thus allowing reliable prediction of spatially continuous fluxes that can capture the cold and hot spots over different seasons across heterogeneous landscapes (Warner et al., 2019; Räsänen et al., 2021). This study's high spatial resolution upscaling (1 m pixel) enabled capturing small-scale variabilities in GHG fluxes within short distances, which would have been missed with coarser resolution upscaling. Upscaling at a finer resolution was especially relevant due to the heterogeneous nature of our study landscape, related to different land uses, soil types, and slope positions.

It is noteworthy that the applicability of this upscaling approach largely depends on the availability of spatially extensive chamber measurements. In this study, the 70% modeling dataset represented data from ~20 stratified chamber locations per km^2 on the arable land and ~16 chambers per km^2 in the forest. These number of chamber measurement locations are within the range of those recommended (29 for arable and 13 for forest) by Wangari et al. (2022) for accurate quantification of landscape GHG fluxes. Based on these findings, these chamber numbers may be adoptable to other studies looking to upscale GHG fluxes using a combination of chamber measurements and remotely-sensed data, but this will highly depend on the level of similarities in landscape properties with our study.

5. Conclusions

This study demonstrated the potential of improved prediction performance when combining field-based measurements of soil parameters with remotely-sensed data in scaling up flux (chamber) measurements from stratified sites. Among the remotely-sensed predictors, Sentinel-2 indices played a more significant role than DEM-derived attributes in upscaling the GHG fluxes across our relatively flat landscape terrain. The high-resolution (1 m pixel size) scaled-up fluxes effectively revealed fine-scale (within a few meters) hot and cold spots of GHG fluxes across a mixed land use landscape in summer and autumn. The N_2O hot spots were more significant sources of GHGs as they contributed 42% of the landscape N_2O fluxes compared to SR/ER_CO_2 and CH_4 emission hotspots, which accounted for 29% and 2% of the landscape CO_2 and CH_4 emissions, respectively. Arable soils, which had higher N_2O fluxes, also had patches with elevated emissions of the three GHGs, especially in areas with high soil moisture content. These findings emphasize the importance of targeted local mitigation measures, especially for agricultural soils, in mitigating landscape GHG fluxes.

While we identified hot and cold spots of soil GHG flux across the Schwingbach landscape through RF modeling, the entire exercise was limited to two measuring campaigns of a few days in two seasons (summer and autumn). For this reason, it is still unclear whether these hot and cold spots persist throughout the year and their overall contribution to the annual landscape GHG flux estimates. Future studies should, therefore, aim at increasing the temporal resolution of similar spatially extensive measurements to at least monthly scales, which, when combined with remotely-sensed data, may be able to create similar landscape flux maps and identify the contribution of GHG hot and cold spots to annual estimates.

Table 3: Comparison with other studies that have upscaled landscape fluxes using the random forest algorithm

Study area	Landscape area (km^2)	Number of sites	Predictor variables	Measurement period	Model algorithm	Type of validation	Prediction period	Land use	Flux	Model validation (r^2)	Location	Reference
Gießen, Central Germany	5.85	268	○ **DEM indices**: *elevation, slope, aspect, TWI & TPI* ○ **Sentinel-2 indices**: *NDVI, GNDVI, & NDMI* ○ **In-situ data**: *soil temperature, moisture, pH, bulk density, NO_3-N, NH_4-N, DOC, TDN, TN, TOC, CN, sand, silt & clay content*	July & September, 2020	Random forest	10-fold repeated cross-validation	Summer (Jul) and autumn (Sep)	Forest, grassland, arable	SR/ER_CO_2	0.57, 0.57, 0.78	50°30'4.23. N, 8°33'2.82. E	This study
								Forest, grassland, arable	CH_4	0.21, 0.30, 0.31		
								Forest, grassland, arable	N_2O	0.15, 0.25, 0.56		
Hyytiälä, southern Finland	0.1	60	○ **DEM indices**: *slope, TWI, TRI & DTW* ○ **In-situ data**: soil moisture	March-December 2013 & May-December 2014	Random forest	Distance-blocked leave-out cross-	Summer Autumn	Forest (boreal)	CH_4	0.26 0.39	61°510 N, 24°170 E	Vainio et al. (2021)
Maryland, USA	0.12	20	○ **DEM indices**: slope, aspect, TWI, flow line curvature, channel network base level, upslope accumulation area,etc. ○ **In-situ data**: *soil temperature & moisture*	September 2014 - November 2016 (bimonthly)	Quantile regression forest	Model accuracy and prediction uncertainity assessment	Early summer: May-Jul Late summer: Aug-Sep	Forest (headwater watershed)	CO_2 & CH_4	0.61, 0.50 (CO_2, CH_4) 0.40, 0.64 (CO_2, CH_4)	39°42′ N, 75°50′ W	Warner et al. (2019)
Pallas area, northern Finland	12.4	279	○ **DEM indices**: *elevation, slope, aspect, TWI, TPI & DTW* ○ **Sentinel-1 & 2 indices**: NDVI, GNDVI, NDWI, etc ○ **In-situ data:** soil moisture, vegetation (e.g., leaf area index)	July 3 - 13, 2019	Random forest regressions and binary classifications	Random forest out-of-bag assessment	Summer (July)	Forest (peatland)	CH_4	0.76	67°57′–68°01′ N, 24°10′ –24°15′ E	Räsänen et al. (2021)
Narrabri, New South Wales, Australia	0.16	>100	○ **RSX-1 Gamma Detector variables**: *clay content, mineralogy, soil pH* ○ **DUALEM–4 s Electromagnetic sensor variables**: *moisture, salinity, clay, thickness of the solum*	May 23-31, 2015	Quantile regression forest	Linear regression with validation dataset	Early summer (May)	Arable	CH_4 & N_2O	0.24, 0.07 (CH_4, N_2O)	149.82° E; 30.28° S	McDaniel et al. (2017)

Appendices

Appendix A: Figures

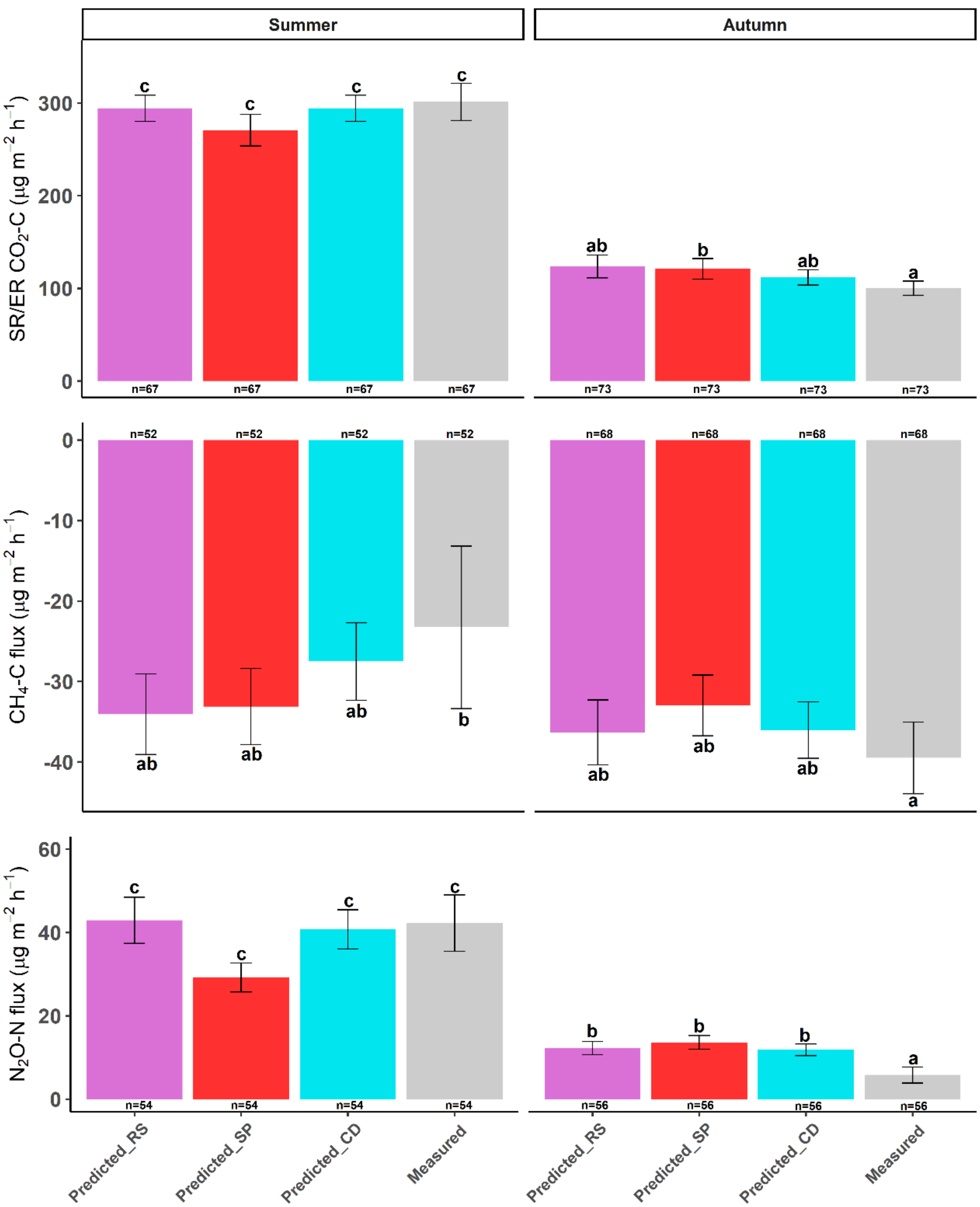

Figure A1: Bar graphs showing the mean fluxes (±SE) predicted using remote sensing (RS), soil properties (SP), and combined data (CD) and the measured fluxes at the sampling sites in the 30% model test dataset. The upper-case and lower-case letters indicate significant differences ($p<0.05$) in the mean fluxes in the different seasons and across the measured and predicted fluxes.

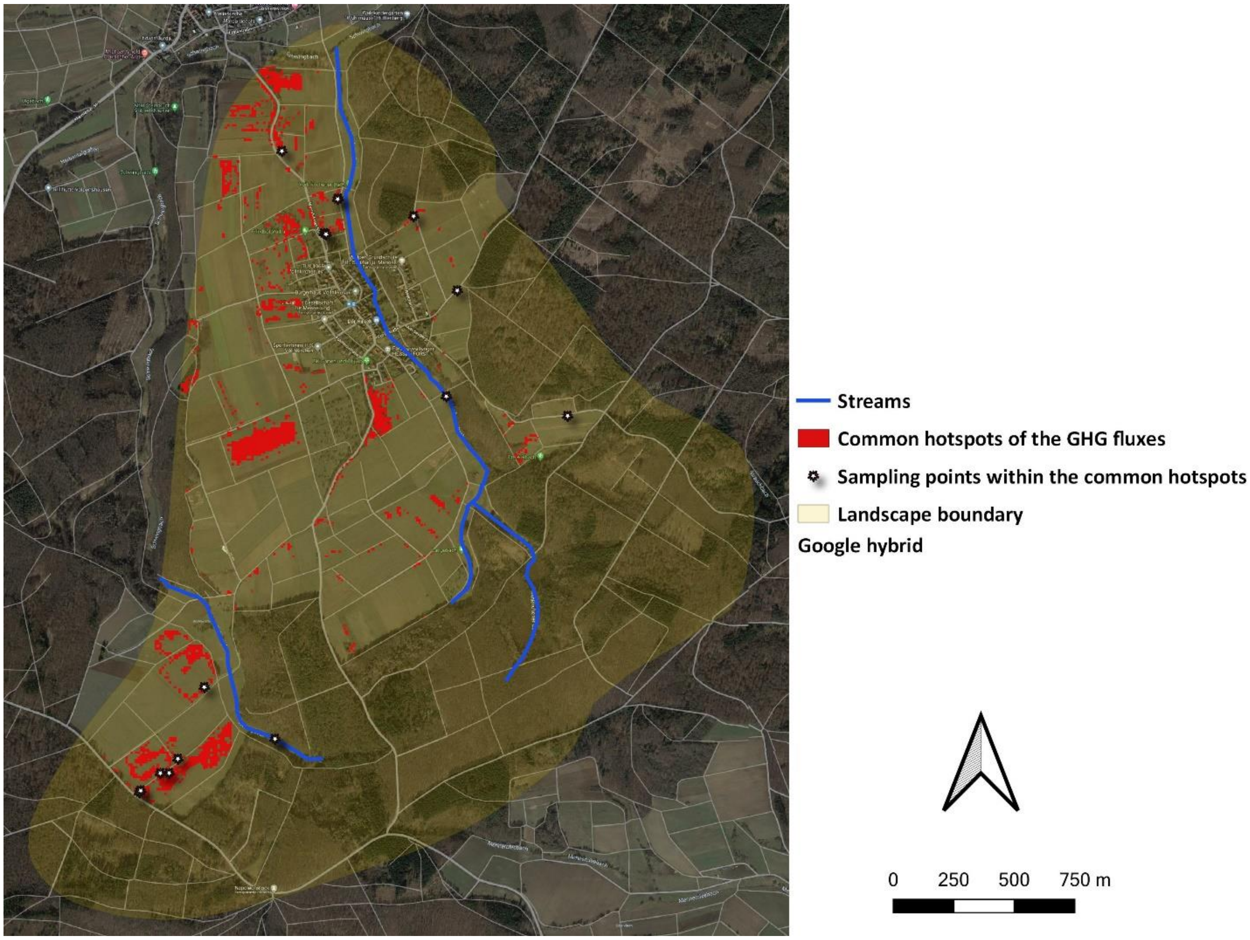

Figure A2: Map showing the common hotspot regions of the three GHG fluxes and the location of the measured sampling points within these recurrent hotspots (Satellite Image downloaded from Google Maps).

Figure A3: Clover (*Trifolium*) on grassland ecosystems.

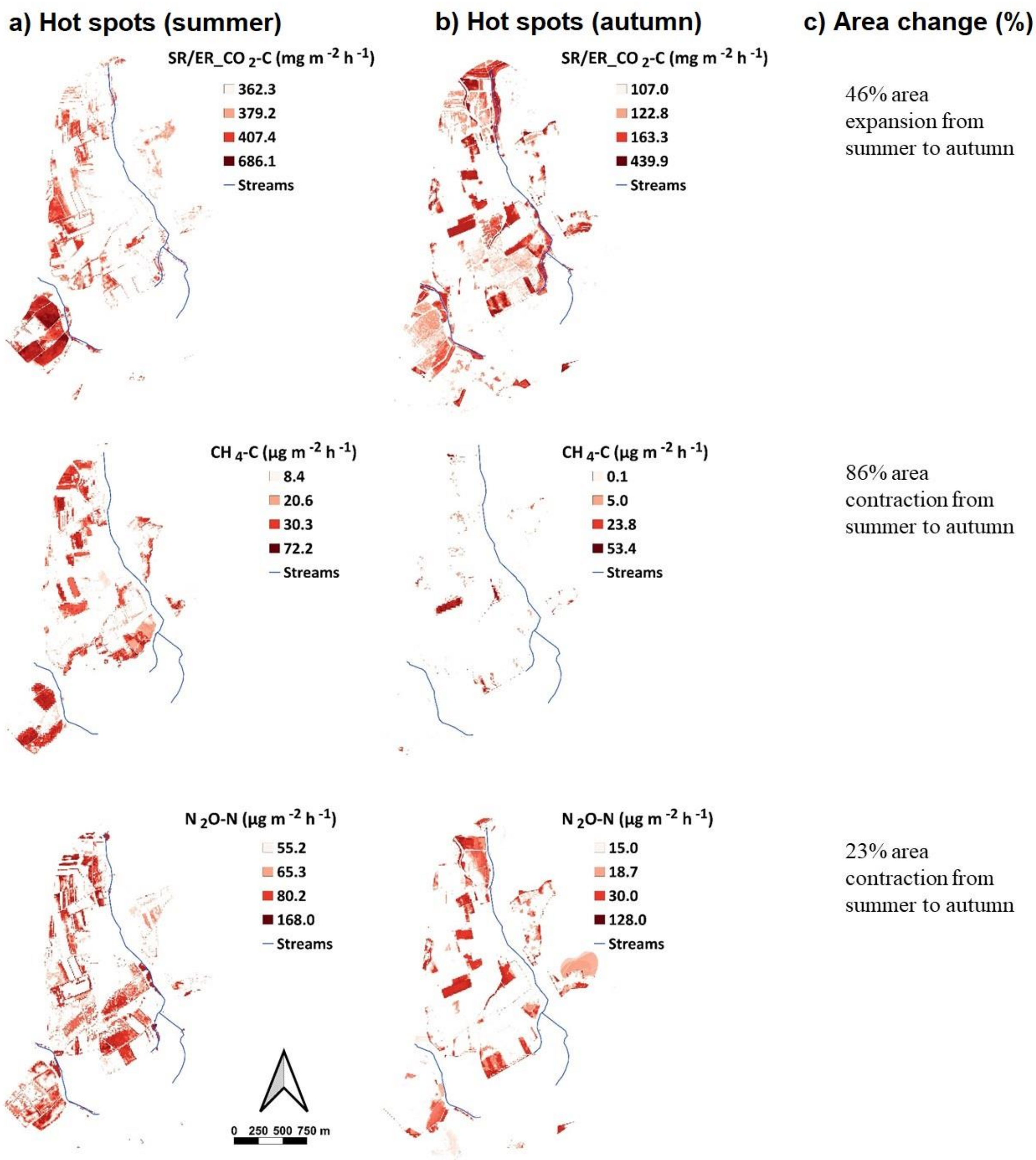

Figure A4: Maps showing the hot spots of the (a) summer and (b) autumn seasons and (c) the percentage change in the area coverage of the hot spots. These regions were defined using each season's specific hot spot threshold.

Appendix B: Tables

Table B1 a, b, c: Cross-validation results of different models developed for SR/ER-CO_2 fluxes in 1a) forest, 1b) grassland and 1c) arable land using different predictors in the training dataset. Stepwise elimination of least important predictors was implemented.

B1a): Forest SR_CO_2-C flux		**10-fold cross validation**			
Category	**Predictor variables**	**mtry**	**RMSE**	**R^2**	**MAE**
Remote sensing	Elevation, slope, aspect, TWI, TPI, NDVI, GNDVI, NDMI	2	1.77	0.44	1.56
	Elevation, aspect, TWI, TPI, NDVI, GNDVI, NDMI	2	1.77	0.43	1.56
	Elevation, aspect, TPI, NDVI, GNDVI, NDMI	2	1.76	0.44	1.56
	Elevation, TPI, NDVI, GNDVI, NDMI	2	1.75	0.46	1.54
	Elevation, NDVI, GNDVI, NDMI	2	1.73	0.48	1.54
	NDVI, GNDVI, NDMI	2	1.76	0.45	1.55
	NDVI, GNDVI	2	1.81	0.42	1.58
	NDVI	2	1.88	0.36	1.63
Site measured soil parameters	Temperature, moisture, pH, bulk density, NO_3-N, NH_4-N, DOC, TDN, SOC, SN, CN, sand, silt, clay	8	1.71	0.50	1.52
	Temperature, moisture, pH, bulk density, NO_3-N, NH_4-N, DOC, TDN, SOC, SN, sand, silt, clay	7	1.70	0.51	1.51
	Temperature, moisture, pH, bulk density, NO_3-N, NH_4-N, DOC, TDN, SOC, SN, sand, silt	7	1.70	0.51	1.51
	Temperature, moisture, pH, bulk density, NH_4-N, DOC, TDN, SOC, SN, sand, silt	6	1.69	0.52	1.50
	Temperature, moisture, pH, bulk density, NH_4-N, DOC, TDN, SN, sand, silt	6	1.69	0.52	1.50
	Temperature, moisture, pH, bulk density, NH_4-N, DOC, TDN, sand, silt	5	1.69	0.52	1.50
	Moisture, pH, bulk density, NH_4-N, DOC, TDN, sand, silt	5	1.70	0.51	1.51
	Moisture, pH, NH_4-N, DOC, TDN, sand, silt	4	1.69	0.52	1.51
	Moisture, pH, NH_4-N, DOC, TDN, silt	2	1.68	0.53	1.51
	Moisture, pH, NH_4-N, DOC, TDN	2	1.70	0.51	1.52
	Moisture, pH, NH_4-N, DOC	2	1.72	0.49	1.53
	Moisture, NH_4-N, DOC	2	1.77	0.44	1.56
	Moisture, NH_4-N	2	1.77	0.44	1.56
	NH_4-N	2	1.82	0.41	1.62
Combined	Elevation, slope, aspect, TWI, TPI, NDVI, GNDVI, NDMI, temperature, moisture, pH, bulk density, NO_3-N, NH_4-N, DOC, TDN, SOC, SN, CN, sand, silt, clay	12	1.67	0.54	1.49
	Slope, aspect, TWI, TPI, NDVI, GNDVI, NDMI, temperature, moisture, pH, bulk density, NO_3-N, NH_4-N, DOC, TDN, SOC, SN, CN, sand, silt, clay	11	1.67	0.54	1.49
	Slope, aspect, TPI, NDVI, GNDVI, NDMI, temperature, moisture, pH, bulk density, NO_3-N, NH_4-N, DOC, TDN, SOC, SN, CN, sand, silt, clay	11	1.66	0.55	1.49
	Aspect, TPI, NDVI, GNDVI, NDMI, temperature, moisture, pH, bulk density, NO_3-N, NH_4-N, DOC, TDN, SOC, SN, CN, sand, silt, clay	10	1.67	0.55	1.49
	TPI, NDVI, GNDVI, NDMI, temperature, moisture, pH, bulk density, NO_3-N, NH_4-N, DOC, TDN, SOC, SN, CN, sand, silt, clay	10	1.67	0.55	1.48
	TPI, NDVI, GNDVI, NDMI, temperature, moisture, pH, bulk density, NO_3-N, NH_4-N, DOC, TDN, SOC, SN, CN, sand, silt	9	1.66	0.56	1.48
	TPI, NDVI, GNDVI, NDMI, temperature, moisture, pH, bulk density, NO_3-N, NH_4-N, DOC, TDN, SOC, SN, sand, silt	2	1.65	0.58	1.48
	NDVI, GNDVI, NDMI, temperature, moisture, pH, bulk density, NO_3-N, NH_4-N, DOC, TDN, SOC, SN, sand, silt	8	1.65	0.56	1.48
	NDVI, GNDVI, NDMI, temperature, moisture, pH, bulk density, NH_4-N, DOC, TDN, SOC, SN, sand, silt	2	1.64	0.59	1.47
	NDVI, GNDVI, NDMI, temperature, moisture, pH, bulk density, NH_4-N, DOC, TDN, SOC, SN, silt	2	1.63	0.60	1.47
	NDVI, GNDVI, NDMI, temperature, moisture, pH, NH_4-N, DOC, TDN, SOC, SN, silt	2	1.63	0.60	1.46
	NDVI, GNDVI, NDMI, temperature, moisture, pH, NH_4-N, DOC, TDN, SOC, silt	2	1.63	0.60	1.46
	NDVI, GNDVI, NDMI, moisture, pH, NH_4-N, DOC, TDN, SOC, silt	2	1.63	0.59	1.47
	NDVI, GNDVI, NDMI, moisture, pH, NH_4-N, DOC, TDN, silt	2	1.63	0.59	1.47
	NDVI, GNDVI, NDMI, moisture, pH, NH_4-N, DOC, TDN	2	1.64	0.57	1.48
	NDVI, GNDVI, NDMI, moisture, NH_4-N, DOC, TDN	2	1.65	0.57	1.48
	NDVI, GNDVI, NDMI, moisture, NH_4-N, DOC	2	1.64	0.57	1.48
	NDVI, GNDVI, moisture, NH_4-N, DOC	2	1.67	0.55	1.49
	NDVI, GNDVI, moisture, NH_4-N	3	1.67	0.55	1.49
	NDVI, moisture, NH_4-N	3	1.68	0.53	1.50
	NDVI, NH_4-N	2	1.69	0.54	1.50
	NH_4-N	2	1.82	0.41	1.62

B1b): Grassland SR/ER_CO_2-C flux

Category	Predictor variables	mtry	RMSE	R^2	MAE
		10-fold cross validation			
Remote sensing	Elevation, slope, aspect, TWI, TPI, NDVI, GNDVI, NDMI	5	1.87	0.47	1.62
	Elevation, slope, aspect, TPI, NDVI, GNDVI, NDMI	2	1.85	0.48	1.61
	Elevation, aspect, TPI, NDVI, GNDVI, NDMI	2	1.85	0.48	1.60
	Elevation, aspect, NDVI, GNDVI, NDMI	2	1.84	0.49	1.59
	Elevation, NDVI, GNDVI, NDMI	2	1.85	0.48	1.59
	NDVI, GNDVI, NDMI	2	1.88	0.46	1.61
	NDVI, GNDVI	2	1.95	0.41	1.67
	GNDVI	2	2.06	0.36	1.72
Site measured soil parameters	Temperature, moisture, pH, bulk density, NO_3-N, NH_4-N, DOC, TDN, SOC, SN, CN, sand, silt, clay	8	1.76	0.56	1.53
	Temperature, moisture, pH, bulk density, NO_3-N, NH_4-N, DOC, TDN, SOC, SN, CN, sand, clay	7	1.75	0.57	1.53
	Temperature, moisture, pH, NO_3-N, NH_4-N, DOC, TDN, SOC, SN, CN, sand, clay	7	1.75	0.57	1.53
	Moisture, pH, NO_3-N, NH_4-N, DOC, TDN, SOC, SN, CN, sand, clay	6	1.76	0.56	1.53
	Moisture, pH, NO_3-N, NH_4-N, DOC, TDN, SOC, SN, CN, clay	6	1.75	0.57	1.53
	Moisture, pH, NO_3-N, NH_4-N, TDN, SOC, SN, CN, clay	5	1.75	0.57	1.53
	Moisture, pH, NO_3-N, NH_4-N, TDN, SOC, SN, CN	5	1.76	0.56	1.54
	Moisture, NO_3-N, NH_4-N, TDN, SOC, SN, CN	2	1.78	0.55	1.55
	Moisture, NH_4-N, TDN, SOC, SN, CN	2	1.79	0.54	1.56
	Moisture, NH_4-N, TDN, SN, CN	2	1.78	0.55	1.55
	Moisture, NH_4-N, TDN, CN	2	1.79	0.54	1.55
	Moisture, NH_4-N, TDN	2	1.79	0.54	1.55
	Moisture, NH_4-N	2	1.83	0.51	1.60
	Moisture	2	1.88	0.46	1.65
Combined	Elevation, slope, aspect, TWI, TPI, NDVI, GNDVI, NDMI, temperature, moisture, pH, bulk density, NO_3-N, NH_4-N, DOC, TDN, SOC, SN, CN, sand, silt, clay	12	1.74	0.58	1.51
	Elevation, slope, aspect, TWI, NDVI, GNDVI, NDMI, temperature, moisture, pH, bulk density, NO_3-N, NH_4-N, DOC, TDN, SOC, SN, CN, sand, silt, clay	11	1.73	0.59	1.50
	Elevation, slope, aspect, NDVI, GNDVI, NDMI, temperature, moisture, pH, bulk density, NO_3-N, NH_4-N, DOC, TDN, SOC, SN, CN, sand, silt, clay	11	1.73	0.59	1.50
	Elevation, aspect, NDVI, GNDVI, NDMI, temperature, moisture, pH, bulk density, NO_3-N, NH_4-N, DOC, TDN, SOC, SN, CN, sand, silt, clay	10	1.73	0.59	1.50
	Elevation, aspect, NDVI, GNDVI, NDMI, temperature, moisture, pH, bulk density, NO_3-N, NH_4-N, DOC, TDN, SOC, SN, CN, sand, clay	10	1.73	0.59	1.50
	Elevation, NDVI, GNDVI, NDMI, temperature, moisture, pH, bulk density, NO_3-N, NH_4-N, DOC, TDN, SOC, SN, CN, sand, clay	9	1.73	0.59	1.50
	Elevation, NDVI, GNDVI, NDMI, temperature, moisture, pH, NO_3-N, NH_4-N, DOC, TDN, SOC, SN, CN, sand, clay	9	1.73	0.59	1.50
	Elevation, NDVI, GNDVI, NDMI, moisture, pH, NO_3-N, NH_4-N, DOC, TDN, SOC, SN, CN, sand, clay	8	1.73	0.59	1.50
	Elevation, NDVI, GNDVI, NDMI, moisture, NO_3-N, NH_4-N, DOC, TDN, SOC, SN, CN, sand, clay	8	1.73	0.59	1.50
	Elevation, NDVI, GNDVI, NDMI, moisture, NO_3-N, NH_4-N, TDN, SOC, SN, CN, sand, clay	7	1.73	0.59	1.50
	Elevation, NDVI, GNDVI, NDMI, moisture, NO_3-N, NH_4-N, TDN, SOC, SN, CN, clay	7	1.74	0.58	1.51
	Elevation, NDVI, GNDVI, NDMI, moisture, NH_4-N, TDN, SOC, SN, CN, clay	6	1.73	0.59	1.51
	Elevation, NDVI, GNDVI, NDMI, moisture, NH_4-N, TDN, SOC, SN, CN	2	1.74	0.59	1.51
	NDVI, GNDVI, NDMI, moisture, NH_4-N, TDN, SOC, SN, CN	2	1.75	0.58	1.52
	NDVI, GNDVI, NDMI, moisture, NH_4-N, TDN, SOC, CN	2	1.74	0.59	1.51
	NDVI, GNDVI, NDMI, moisture, NH_4-N, TDN, CN	2	1.73	0.59	1.50
	NDVI, GNDVI, moisture, NH_4-N, TDN, CN	2	1.73	0.59	1.51
	NDVI, GNDVI, moisture, NH_4-N, CN	2	1.74	0.58	1.52
	NDVI, GNDVI, moisture, NH_4-N	2	1.74	0.59	1.53
	GNDVI, moisture, NH_4-N	2	1.76	0.57	1.54
	GNDVI, moisture	2	1.84	0.50	1.59
	Moisture	2	1.88	0.46	1.65

B1c): Arable SR/ER_CO_2-C flux **10-fold cross validation**

Category	Predictor variables	mtry	RMSE	R^2	MAE
Remote sensing	Elevation, slope, aspect, TWI, TPI, NDVI, GNDVI, NDMI	8	1.72	0.75	1.55
	Elevation, slope, aspect, TPI, NDVI, GNDVI, NDMI	7	1.72	0.75	1.55
	Elevation, slope, aspect, NDVI, GNDVI, NDMI	4	1.72	0.75	1.55
	Elevation, aspect, NDVI, GNDVI, NDMI	3	1.73	0.75	1.55
	Elevation, NDVI, GNDVI, NDMI	2	1.76	0.73	1.58
	NDVI, GNDVI, NDMI	2	1.80	0.72	1.59
	NDVI, GNDVI	2	1.82	0.71	1.61
	GNDVI	2	1.83	0.71	1.63
Site measured soil parameters	Temperature, moisture, pH, bulk density, NO_3-N, NH_4-N, DOC, TDN, SOC, SN, CN, sand, silt, clay	14	2.00	0.59	1.76
	Temperature, moisture, pH, bulk density, NO_3-N, NH_4-N, DOC, SOC, SN, CN, sand, silt, clay	13	1.99	0.60	1.76
	Temperature, moisture, pH, NO_3-N, NH_4-N, DOC, SOC, SN, CN, sand, silt, clay	12	1.97	0.61	1.74
	Temperature, moisture, pH, NO_3-N, NH_4-N, SOC, SN, CN, sand, silt, clay	11	1.96	0.61	1.74
	Temperature, moisture, pH, NH_4-N, SOC, SN, CN, sand, silt, clay	10	1.96	0.61	1.74
	Temperature, moisture, pH, NH_4-N, SOC, SN, CN, sand, clay	9	1.96	0.61	1.74
	Moisture, pH, NH_4-N, SOC, SN, CN, sand, clay	8	1.95	0.62	1.72
	Moisture, pH, NH_4-N, SN, CN, sand, clay	7	1.94	0.62	1.72
	Moisture, pH, NH_4-N, SN, CN, sand	6	1.94	0.62	1.71
	Moisture, NH_4-N, SN, CN, sand	5	1.93	0.63	1.70
	Moisture, SN, CN, sand	4	1.93	0.63	1.70
	Moisture, SN, CN	3	1.88	0.66	1.67
	Moisture, SN	2	1.94	0.63	1.70
	Moisture	2	2.16	0.50	1.89
Combined	Elevation, slope, aspect, TWI, TPI, NDVI, GNDVI, NDMI, temperature, moisture, pH, bulk density, NO_3-N, NH_4-N, DOC, TDN, SOC, SN, CN, sand, silt, clay	12	1.70	0.77	1.53
	Elevation, aspect, TWI, TPI, NDVI, GNDVI, NDMI, temperature, moisture, pH, bulk density, NO_3-N, NH_4-N, DOC, TDN, SOC, SN, CN, sand, silt, clay	11	1.70	0.77	1.53
	Elevation, aspect, TWI, NDVI, GNDVI, NDMI, temperature, moisture, pH, bulk density, NO_3-N, NH_4-N, DOC, TDN, SOC, SN, CN, sand, silt, clay	11	1.70	0.77	1.53
	Elevation, aspect, NDVI, GNDVI, NDMI, temperature, moisture, pH, bulk density, NO_3-N, NH_4-N, DOC, TDN, SOC, SN, CN, sand, silt, clay	10	1.70	0.77	1.53
	Elevation, aspect, NDVI, GNDVI, NDMI, temperature, moisture, pH, bulk density, NO_3-N, NH_4-N, DOC, SOC, SN, CN, sand, silt, clay	10	1.70	0.77	1.53
	Elevation, aspect, NDVI, GNDVI, NDMI, temperature, moisture, pH, NO_3-N, NH_4-N, DOC, SOC, SN, CN, sand, silt, clay	17	1.69	0.77	1.52
	Elevation, aspect, NDVI, GNDVI, NDMI, temperature, moisture, pH, NO_3-N, NH_4-N, DOC, SOC, SN, CN, sand, clay	16	1.68	0.77	1.52
	Elevation, aspect, NDVI, GNDVI, NDMI, temperature, moisture, pH, NO_3-N, NH_4-N, DOC, SOC, SN, sand, clay	8	1.68	0.78	1.51
	Elevation, aspect, NDVI, GNDVI, NDMI, temperature, moisture, pH, NO_3-N, NH_4-N, DOC, SOC, SN, sand	8	1.68	0.78	1.51
	Elevation, aspect, NDVI, GNDVI, NDMI, temperature, moisture, pH, NH_4-N, DOC, SOC, SN, sand	7	1.68	0.78	1.51
	Elevation, aspect, NDVI, GNDVI, NDMI, temperature, moisture, pH, NH_4-N, SOC, SN, sand	7	1.68	0.78	1.51
	Elevation, aspect, NDVI, GNDVI, NDMI, moisture, pH, NH_4-N, SOC, SN, sand	6	1.67	0.78	1.50
	Elevation, aspect, NDVI, GNDVI, NDMI, moisture, pH, SOC, SN, sand	6	1.67	0.78	1.50
	Elevation, aspect, NDVI, GNDVI, NDMI, moisture, SOC, SN, sand	5	1.66	0.78	1.50
	Elevation, aspect, NDVI, GNDVI, NDMI, moisture, SOC, SN	5	1.66	0.79	1.49
	Elevation, aspect, NDVI, GNDVI, NDMI, moisture, SN	7	1.66	0.79	1.50
	Elevation, aspect, NDVI, GNDVI, moisture, SN	2	1.64	0.80	1.48
	Elevation, NDVI, GNDVI, moisture, SN	2	1.67	0.79	1.51
	NDVI, GNDVI, moisture, SN	2	1.68	0.78	1.51
	NDVI, GNDVI, moisture	2	1.72	0.75	1.54
	NDVI, GNDVI	2	1.82	0.71	1.61
	GNDVI	2	1.83	0.71	1.63

Table B2 a, b, c: Cross-validation results of different models developed for all (positive and negative) CH_4 fluxes in 2a) forest, 2b) grassland and 2c) arable land using different predictors in the training dataset. Stepwise elimination of least important predictors was implemented.

B2a): Forest CH_4-C (positive & negative) flux

		10-fold cross validation			
Category	**Predictor variables**	**mtry**	**RMSE**	**R^2**	**MAE**
Remote sensing	Elevation, slope, aspect, TWI, TPI, NDVI, GNDVI, NDMI	2	45.35	0.13	36.00
	Elevation, slope, aspect, TPI, NDVI, GNDVI, NDMI	2	45.26	0.13	35.97
	Elevation, aspect, TPI, NDVI, GNDVI, NDMI	2	45.07	0.15	35.75
	Elevation, aspect, NDVI, GNDVI, NDMI	2	44.63	0.15	35.00
	Aspect, NDVI, GNDVI, NDMI	2	44.79	0.16	35.37
	Aspect, NDVI, GNDVI	2	46.38	0.14	36.15
	Aspect, NDVI	2	47.90	0.12	37.92
	Aspect	2	54.06	0.07	41.44
Site measured soil parameters	Temperature, moisture, pH, bulk density, NO_3-N, NH_4-N, DOC, TDN, SOC, SN, CN, sand, silt, clay	2	44.79	0.16	34.46
	Temperature, moisture, pH, bulk density, NO_3-N, NH_4-N, DOC, SOC, SN, CN, sand, silt, clay	2	44.65	0.16	34.36
	Temperature, moisture, pH, NO_3-N, NH_4-N, DOC, SOC, SN, CN, sand, silt, clay	2	44.52	0.17	34.28
	Temperature, moisture, pH, NO_3-N, NH_4-N, DOC, SOC, SN, CN, sand, silt	2	44.67	0.16	34.36
	Temperature, moisture, pH, NO_3-N, NH_4-N, DOC, SOC, CN, sand, silt	2	44.54	0.16	34.22
	Temperature, moisture, pH, NO_3-N, NH_4-N, DOC, SOC, sand, silt	2	43.98	0.18	33.93
	Temperature, moisture, pH, NO_3-N, DOC, SOC, sand, silt	2	43.64	0.19	33.73
	Temperature, moisture, pH, NO_3-N, DOC, sand, silt	2	43.46	0.19	33.49
	Temperature, moisture, pH, NO_3-N, sand, silt	2	43.07	0.20	33.20
	Temperature, moisture, pH, NO_3-N, silt	2	44.29	0.16	33.87
	Temperature, moisture, pH, NO_3-N	2	45.84	0.14	35.18
	Temperature, moisture, NO_3-N	2	45.31	0.15	35.40
	Moisture, NO_3-N	2	47.94	0.12	36.80
	Moisture	2	51.25	0.08	40.58
Combined	Elevation, slope, aspect, TWI, TPI, NDVI, GNDVI, NDMI, temperature, moisture, pH, bulk density, NO_3-N, NH_4-N, DOC, TDN, SOC, SN, CN, sand, silt, clay	2	44.31	0.17	34.18
	Elevation, slope, aspect, TWI, TPI, NDVI, GNDVI, NDMI, temperature, moisture, pH, bulk density, NO_3-N, NH_4-N, DOC, TDN, SOC, CN, sand, silt, clay	2	44.37	0.17	34.29
	Elevation, aspect, TWI, TPI, NDVI, GNDVI, NDMI, temperature, moisture, pH, bulk density, NO_3-N, NH_4-N, DOC, TDN, SOC, CN, sand, silt, clay	2	44.23	0.18	34.15
	Elevation, aspect, TPI, NDVI, GNDVI, NDMI, temperature, moisture, pH, bulk density, NO_3-N, NH_4-N, DOC, TDN, SOC, CN, sand, silt, clay	2	44.05	0.19	34.05
	Elevation, aspect, NDVI, GNDVI, NDMI, temperature, moisture, pH, bulk density, NO_3-N, NH_4-N, DOC, TDN, SOC, CN, sand, silt, clay	2	43.90	0.19	33.99
	Elevation, aspect, NDVI, GNDVI, NDMI, temperature, moisture, pH, NO_3-N, NH_4-N, DOC, TDN, SOC, CN, sand, silt, clay	2	43.80	0.19	33.88
	Elevation, aspect, NDVI, GNDVI, NDMI, temperature, moisture, pH, NO_3-N, NH_4-N, DOC, SOC, CN, sand, silt, clay	2	43.60	0.20	33.74
	Elevation, aspect, NDVI, GNDVI, NDMI, temperature, moisture, pH, NO_3-N, NH_4-N, DOC, SOC, CN, sand, silt	2	43.64	0.20	33.88
	Elevation, aspect, NDVI, GNDVI, temperature, moisture, pH, NO_3-N, NH_4-N, DOC, SOC, CN, sand, silt	2	43.51	0.20	33.78
	Aspect, NDVI, GNDVI, temperature, moisture, pH, NO_3-N, NH_4-N, DOC, SOC, CN, sand, silt	2	43.48	0.20	33.79
	Aspect, NDVI, GNDVI, temperature, moisture, pH, NO_3-N, DOC, SOC, CN, sand, silt	2	43.03	0.22	33.48
	Aspect, NDVI, GNDVI, temperature, moisture, pH, NO_3-N, DOC, CN, sand, silt	2	42.76	0.22	33.17
	Aspect, NDVI, GNDVI, temperature, moisture, pH, NO_3-N, DOC, CN, silt	2	43.24	0.20	33.49
	Aspect, NDVI, GNDVI, temperature, moisture, pH, NO_3-N, DOC, silt	2	42.81	0.21	33.41
	Aspect, NDVI, GNDVI, temperature, moisture, pH, NO_3-N, silt	2	42.49	0.23	33.30
	Aspect, GNDVI, temperature, moisture, pH, NO_3-N, silt	2	42.71	0.22	33.42
	Aspect, temperature, moisture, pH, NO_3-N, silt	2	43.29	0.20	33.83
	Aspect, temperature, moisture, pH, NO_3-N	2	43.92	0.19	34.69
	Aspect, temperature, moisture, NO_3-N	2	43.50	0.21	34.58
	Temperature, moisture, NO_3-N	2	45.31	0.15	35.40
	Moisture, NO_3-N	2	47.94	0.12	36.80
	Moisture	2	51.25	0.08	40.58

B2b): Grassland CH_4-C (positive & negative) flux

Category	Predictor variables	10-fold cross validation			
Category	**Predictor variables**	**mtry**	**RMSE**	**R^2**	**MAE**
Remote sensing	Elevation, slope, aspect, TWI, TPI, NDVI, GNDVI, NDMI	2	28.88	0.15	20.98
	Elevation, slope, aspect, TPI, NDVI, GNDVI, NDMI	2	28.73	0.16	20.97
	Elevation, aspect, TPI, NDVI, GNDVI, NDMI	2	29.19	0.15	21.54
	Elevation, TPI, NDVI, GNDVI, NDMI	2	28.85	0.14	21.56
	Elevation, TPI, NDVI, NDMI	2	29.23	0.15	21.53
	Elevation, TPI, NDMI	2	30.08	0.14	22.04
	Elevation, NDMI	2	30.46	0.13	22.57
	Elevation	2	30.72	0.13	22.84
Site measured soil parameters	Temperature, moisture, pH, bulk density, NO_3-N, NH_4-N, DOC, TDN, SOC, SN, CN, sand, silt, clay	2	26.98	0.22	19.52
	Temperature, moisture, pH, bulk density, NO_3-N, NH_4-N, DOC, TDN, SOC, SN, CN, silt, clay	7	26.96	0.22	19.42
	Temperature, moisture, pH, bulk density, NO_3-N, NH_4-N, DOC, TDN, SN, CN, silt, clay	7	26.86	0.23	19.38
	Temperature, moisture, pH, bulk density, NO_3-N, NH_4-N, DOC, TDN, SN, CN, clay	6	26.66	0.23	19.20
	Temperature, moisture, pH, bulk density, NO_3-N, NH_4-N, DOC, TDN, CN, clay	6	26.68	0.23	19.28
	Temperature, moisture, pH, NO_3-N, NH_4-N, DOC, TDN, CN, clay	5	26.60	0.24	19.16
	Temperature, moisture, pH, NO_3-N, DOC, TDN, CN, clay	2	26.27	0.25	19.00
	Moisture, pH, NO_3-N, DOC, TDN, CN, clay	2	26.16	0.26	19.01
	Moisture, pH, NO_3-N, DOC, CN, clay	2	25.59	0.29	18.62
	Moisture, pH, NO_3-N, DOC, CN	2	26.27	0.25	19.58
	Moisture, pH, DOC, CN	2	26.81	0.23	19.51
	Moisture, DOC, CN	2	26.96	0.24	20.19
	Moisture, CN	2	28.73	0.23	21.43
	Moisture	2	30.95	0.14	23.49
Combined	Elevation, slope, aspect, TWI, TPI, NDVI, GNDVI, NDMI, temperature, moisture, pH, bulk density, NO_3-N, NH_4-N, DOC, TDN, SOC, SN, CN, sand, silt, clay	12	26.91	0.22	19.51
	Elevation, slope, TWI, TPI, NDVI, GNDVI, NDMI, temperature, moisture, pH, bulk density, NO_3-N, NH_4-N, DOC, TDN, SOC, SN, CN, sand, silt, clay	2	26.89	0.22	19.42
	Elevation, slope, TWI, TPI, NDVI, GNDVI, NDMI, temperature, moisture, pH, bulk density, NO_3-N, NH_4-N, DOC, TDN, SOC, SN, CN, sand, clay	2	26.74	0.23	19.36
	Elevation, slope, TWI, TPI, NDVI, GNDVI, NDMI, temperature, moisture, pH, bulk density, NO_3-N, NH_4-N, DOC, TDN, SN, CN, sand, clay	10	26.71	0.23	19.30
	Elevation, slope, TWI, TPI, NDVI, NDMI, temperature, moisture, pH, bulk density, NO_3-N, NH_4-N, DOC, TDN, SN, CN, sand, clay	2	26.56	0.24	19.22
	Elevation, TWI, TPI, NDVI, NDMI, temperature, moisture, pH, bulk density, NO_3-N, NH_4-N, DOC, TDN, SN, CN, sand, clay	2	26.68	0.23	19.39
	Elevation, TPI, NDVI, NDMI, temperature, moisture, pH, bulk density, NO_3-N, NH_4-N, DOC, TDN, SN, CN, sand, clay	2	26.75	0.22	19.36
	Elevation, TPI, NDVI, NDMI, temperature, moisture, pH, bulk density, NO_3-N, NH_4-N, DOC, TDN, SN, CN, clay	2	26.62	0.23	19.29
	Elevation, TPI, NDVI, NDMI, temperature, moisture, pH, bulk density, NO_3-N, NH_4-N, DOC, TDN, CN, clay	2	26.77	0.22	19.35
	Elevation, TPI, NDVI, NDMI, temperature, moisture, pH, NO_3-N, NH_4-N, DOC, TDN, CN, clay	2	26.65	0.23	19.27
	Elevation, TPI, NDVI, NDMI, moisture, pH, NO_3-N, NH_4-N, DOC, TDN, CN, clay	2	26.69	0.22	19.39
	Elevation, TPI, NDVI, NDMI, moisture, pH, NO_3-N, DOC, TDN, CN, clay	2	26.45	0.24	19.29
	Elevation, TPI, NDMI, moisture, pH, NO_3-N, DOC, TDN, CN, clay	2	26.30	0.24	19.14
	TPI, NDMI, moisture, pH, NO_3-N, DOC, TDN, CN, clay	2	26.33	0.25	19.16
	TPI, NDMI, moisture, pH, NO_3-N, DOC, CN, clay	2	25.91	0.27	18.85
	TPI, NDMI, moisture, pH, NO_3-N, CN, clay	2	25.83	0.27	18.62
	TPI, moisture, pH, NO_3-N, CN, clay	2	25.32	0.31	18.18
	Moisture, pH, NO_3-N, CN, clay	2	25.38	0.30	18.29
	Moisture, pH, NO_3-N, CN	2	26.65	0.25	19.61
	Moisture, pH, NO_3-N	2	27.60	0.19	20.52
	Moisture, pH	2	29.67	0.14	22.56
	Moisture	2	30.95	0.14	23.49

B2c): Arable CH_4-C (positive & negative) flux

Category	Predictor variables	10-fold cross validation			
		mtry	RMSE	R^2	MAE
Remote sensing	Elevation, slope, aspect, TWI, TPI, NDVI, GNDVI, NDMI	2	48.58	0.28	33.46
	Elevation, slope, aspect, TWI, NDVI, GNDVI, NDMI	2	48.10	0.28	33.16
	Elevation, slope, aspect, NDVI, GNDVI, NDMI	2	48.79	0.29	33.46
	Elevation, aspect, NDVI, GNDVI, NDMI	2	49.56	0.29	33.54
	Aspect, NDVI, GNDVI, NDMI	2	47.59	0.25	32.46
	Aspect, GNDVI, NDMI	2	48.56	0.26	33.18
	GNDVI, NDMI	2	50.79	0.35	34.72
	NDMI	2	52.71	0.30	36.62
Site measured soil parameters	Temperature, moisture, pH, bulk density, NO_3-N, NH_4-N, DOC, TDN, SOC, SN, CN, sand, silt, clay	2	45.46	0.24	32.35
	Temperature, moisture, pH, bulk density, NO_3-N, NH_4-N, DOC, TDN, SOC, SN, CN, silt, clay	2	45.74	0.22	32.67
	Temperature, moisture, pH, bulk density, NO_3-N, DOC, TDN, SOC, SN, CN, silt, clay	2	45.73	0.21	32.67
	Temperature, moisture, pH, bulk density, NO_3-N, DOC, TDN, SOC, SN, CN, clay	2	45.79	0.21	32.53
	Temperature, moisture, pH, bulk density, NO_3-N, DOC, SOC, SN, CN, clay	2	46.74	0.21	33.25
	Temperature, pH, bulk density, NO_3-N, DOC, SOC, SN, CN, clay	2	46.81	0.21	33.69
	pH, bulk density, NO_3-N, DOC, SOC, SN, CN, clay	2	46.64	0.23	33.38
	pH, bulk density, NO_3-N, DOC, SOC, CN, clay	2	45.99	0.23	33.22
	Bulk density, NO_3-N, DOC, SOC, CN, clay	2	45.03	0.27	31.97
	Bulk density, NO_3-N, DOC, SOC, CN	2	44.43	0.28	32.08
	Bulk density, NO_3-N, DOC, CN	2	44.16	0.25	31.82
	NO_3-N, DOC, CN	2	43.73	0.30	31.45
	DOC, CN	2	44.51	0.29	32.65
	CN	2	45.77	0.28	34.09
Combined	Elevation, slope, aspect, TWI, TPI, NDVI, GNDVI, NDMI, temperature, moisture, pH, bulk density, NO_3-N, NH_4-N, DOC, TDN, SOC, SN, CN, sand, silt, clay	2	46.85	0.23	33.13
	Elevation, slope, aspect, TWI, TPI, NDVI, GNDVI, NDMI, temperature, moisture, pH, bulk density, NO_3-N, DOC, TDN, SOC, SN, CN, sand, silt, clay	2	46.91	0.21	33.19
	Elevation, slope, aspect, TWI, NDVI, GNDVI, NDMI, temperature, moisture, pH, bulk density, NO_3-N, DOC, TDN, SOC, SN, CN, sand, silt, clay	2	46.60	0.22	32.99
	Elevation, slope, aspect, NDVI, GNDVI, NDMI, temperature, moisture, pH, bulk density, NO_3-N, DOC, TDN, SOC, SN, CN, sand, silt, clay	2	46.83	0.22	33.03
	Elevation, slope, aspect, NDVI, GNDVI, NDMI, temperature, moisture, pH, bulk density, NO_3-N, DOC, TDN, SOC, SN, CN, sand, clay	2	46.87	0.23	33.01
	Elevation, slope, aspect, NDVI, GNDVI, NDMI, temperature, moisture, pH, bulk density, NO_3-N, DOC, TDN, SOC, SN, CN, clay	2	47.11	0.25	33.25
	Elevation, aspect, NDVI, GNDVI, NDMI, temperature, moisture, pH, bulk density, NO_3-N, DOC, TDN, SOC, SN, CN, clay	2	46.86	0.23	32.89
	Elevation, aspect, NDVI, GNDVI, NDMI, temperature, moisture, pH, bulk density, NO_3-N, DOC, SOC, SN, CN, clay	2	47.79	0.26	33.60
	Elevation, aspect, NDVI, GNDVI, NDMI, temperature, moisture, pH, bulk density, NO_3-N, DOC, SOC, CN, clay	2	47.86	0.25	33.69
	Elevation, aspect, NDVI, GNDVI, NDMI, moisture, pH, bulk density, NO_3-N, DOC, SOC, CN, clay	2	47.62	0.25	33.38
	Elevation, aspect, NDVI, GNDVI, NDMI, pH, bulk density, NO_3-N, DOC, SOC, CN, clay	2	47.28	0.24	33.32
	Elevation, aspect, NDVI, GNDVI, NDMI, pH, bulk density, NO_3-N, DOC, SOC, CN	2	46.41	0.22	32.75
	Elevation, aspect, NDVI, GNDVI, NDMI, pH, NO_3-N, DOC, SOC, CN	2	46.44	0.22	32.65
	Elevation, aspect, NDVI, GNDVI, NDMI, pH, NO_3-N, DOC, CN	2	46.67	0.23	32.67
	Elevation, aspect, GNDVI, NDMI, pH, NO_3-N, DOC, CN	2	46.47	0.23	32.76
	Elevation, aspect, GNDVI, NDMI, pH, NO_3-N, CN	2	47.43	0.25	33.18
	Elevation, aspect, GNDVI, NDMI, pH, CN	2	47.10	0.25	32.74
	Elevation, aspect, GNDVI, NDMI, CN	3	47.49	0.26	32.67
	Aspect, GNDVI, NDMI, CN	2	46.05	0.23	31.87
	GNDVI, NDMI, CN	2	47.59	0.31	33.30
	NDMI, CN	2	47.29	0.24	33.50
	CN	2	45.77	0.28	34.09

Table B3 a, b, c: Cross-validation results of different models developed for all (positive and negative) N_2O fluxes in 3a) forest, 3b) grassland and 3c) arable land using different predictors in the training dataset. Stepwise elimination of least important predictors was implemented.

B3a): Forest N_2O-N (positive & negative) flux		**10-fold cross validation**			
Category	**Predictor variables**	**mtry**	**RMSE**	**R^2**	**MAE**
Remote sensing	Elevation, slope, aspect, TWI, TPI, NDVI, GNDVI, NDMI	2	18.47	0.11	18.65
	Elevation, aspect, TWI, TPI, NDVI, GNDVI, NDMI	2	18.47	0.11	18.65
	Elevation, aspect, TPI, NDVI, GNDVI, NDMI	2	18.48	0.11	18.65
	Elevation, aspect, NDVI, GNDVI, NDMI	2	18.46	0.09	18.63
	Aspect, NDVI, GNDVI, NDMI	2	18.44	0.12	18.61
	NDVI, GNDVI, NDMI	2	18.46	0.13	18.62
	NDVI, GNDVI	2	18.43	0.11	18.61
	GNDVI	2	18.41	0.12	18.59
Site measured soil parameters	Temperature, moisture, pH, bulk density, NO_3-N, NH_4-N, DOC, TDN, SOC, SN, CN, sand, silt, clay	2	18.49	0.12	18.66
	Temperature, moisture, bulk density, NO_3-N, NH_4-N, DOC, TDN, SOC, SN, CN, sand, silt, clay	2	18.49	0.12	18.66
	Temperature, moisture, bulk density, NO_3-N, NH_4-N, DOC, TDN, SOC, SN, CN, sand, silt	2	18.49	0.13	18.67
	Temperature, moisture, bulk density, NO_3-N, NH_4-N, DOC, TDN, SOC, SN, CN, silt	2	18.49	0.14	18.67
	Temperature, moisture, NO_3-N, NH_4-N, DOC, TDN, SOC, SN, CN, silt	2	18.49	0.13	18.67
	Temperature, moisture, NO_3-N, NH_4-N, DOC, TDN, SOC, SN, silt	2	18.49	0.12	18.66
	Temperature, moisture, NO_3-N, NH_4-N, DOC, TDN, SN, silt	2	18.49	0.13	18.67
	Temperature, moisture, NO_3-N, NH_4-N, TDN, SN, silt	2	18.49	0.15	18.67
	Temperature, moisture, NO_3-N, NH_4-N, TDN, SN	2	18.49	0.15	18.66
	Temperature, moisture, NO_3-N, NH_4-N, TDN	2	18.48	0.15	18.66
	Temperature, moisture, NO_3-N, NH_4-N	2	18.48	0.13	18.65
	Moisture, NO_3-N, NH_4-N	2	18.49	0.15	18.65
	Moisture, NO_3-N	2	18.43	0.11	18.60
	NO_3-N	2	18.38	0.11	18.59
Combined	Elevation, slope, aspect, TWI, TPI, NDVI, GNDVI, NDMI, temperature, moisture, pH, bulk density, NO_3-N, NH_4-N, DOC, TDN, SOC, SN, CN, sand, silt, clay	2	18.49	0.11	18.67
	Elevation, slope, aspect, TWI, TPI, NDVI, GNDVI, NDMI, temperature, moisture, bulk density, NO_3-N, NH_4-N, DOC, TDN, SOC, SN, CN, sand, silt, clay	2	18.49	0.13	18.67
	Elevation, aspect, TWI, TPI, NDVI, GNDVI, NDMI, temperature, moisture, bulk density, NO_3-N, NH_4-N, DOC, TDN, SOC, SN, CN, sand, silt, clay	2	18.49	0.12	18.67
	Elevation, aspect, TPI, NDVI, GNDVI, NDMI, temperature, moisture, bulk density, NO_3-N, NH_4-N, DOC, TDN, SOC, SN, CN, sand, silt, clay	2	18.49	0.12	18.67
	Elevation, aspect, NDVI, GNDVI, NDMI, temperature, moisture, bulk density, NO_3-N, NH_4-N, DOC, TDN, SOC, SN, CN, sand, silt, clay	2	18.49	0.12	18.67
	Elevation, aspect, NDVI, GNDVI, NDMI, temperature, moisture, bulk density, NO_3-N, NH_4-N, DOC, TDN, SOC, SN, CN, sand, silt	2	18.49	0.12	18.67
	Elevation, aspect, NDVI, GNDVI, NDMI, temperature, moisture, bulk density, NO_3-N, NH_4-N, DOC, TDN, SOC, SN, CN, silt	2	18.49	0.13	18.67
	Elevation, aspect, NDVI, GNDVI, NDMI, temperature, moisture, NO_3-N, NH_4-N, DOC, TDN, SOC, SN, CN, silt	2	18.49	0.12	18.67
	Elevation, aspect, NDVI, GNDVI, temperature, moisture, NO_3-N, NH_4-N, DOC, TDN, SOC, SN, CN, silt	2	18.49	0.13	18.67
	Elevation, aspect, GNDVI, temperature, moisture, NO_3-N, NH_4-N, DOC, TDN, SOC, SN, CN, silt	2	18.50	0.13	18.67
	Elevation, aspect, temperature, moisture, NO_3-N, NH_4-N, DOC, TDN, SOC, SN, CN, silt	2	18.49	0.13	18.67
	Aspect, temperature, moisture, NO_3-N, NH_4-N, DOC, TDN, SOC, SN, CN, silt	2	18.49	0.13	18.67
	Aspect, temperature, moisture, NO_3-N, NH_4-N, DOC, TDN, SN, CN, silt	2	18.49	0.13	18.67
	Aspect, temperature, moisture, NO_3-N, NH_4-N, DOC, TDN, SN, CN	2	18.49	0.14	18.67
	Aspect, temperature, moisture, NO_3-N, NH_4-N, DOC, TDN, SN	2	18.49	0.15	18.67
	Aspect, temperature, moisture, NO_3-N, NH_4-N, TDN, SN	2	18.49	0.16	18.67
	Aspect, temperature, moisture, NO_3-N, NH_4-N, TDN	2	18.48	0.16	18.66
	Temperature, moisture, NO_3-N, NH_4-N, TDN	2	18.48	0.15	18.66
	Temperature, moisture, NO_3-N, NH_4-N	2	18.48	0.13	18.65
	Moisture, NO_3-N, NH_4-N	2	18.49	0.15	18.65
	Moisture, NO_3-N	2	18.43	0.11	18.60
	NO_3-N	2	18.38	0.11	18.59

B3b): Grassland N_2O-N (positive & negative) flux

Category	Predictor variables	10-fold cross validation			
		mtry	RMSE	R^2	MAE
Remote sensing	Elevation, slope, aspect, TWI, TPI, NDVI, GNDVI, NDMI	2	17.92	0.13	18.30
	Elevation, slope, aspect, TPI, NDVI, GNDVI, NDMI	2	17.93	0.13	18.30
	Elevation, aspect, TPI, NDVI, GNDVI, NDMI	2	17.90	0.12	18.27
	Elevation, aspect, NDVI, GNDVI, NDMI	2	17.90	0.14	18.29
	Elevation, NDVI, GNDVI, NDMI	2	17.91	0.14	18.27
	NDVI, GNDVI, NDMI	2	17.87	0.13	18.26
	NDVI, NDMI	2	17.87	0.11	18.23
	NDVI	2	17.81	0.11	18.16
Site measured soil parameters	Temperature, moisture, pH, bulk density, NO_3-N, NH_4-N, DOC, TDN, SOC, SN, CN, sand, silt, clay	2	17.95	0.12	18.35
	Temperature, moisture, pH, NO_3-N, NH_4-N, DOC, TDN, SOC, SN, CN, sand, silt, clay	2	17.95	0.12	18.36
	Temperature, moisture, pH, NO_3-N, NH_4-N, DOC, TDN, SOC, SN, CN, sand, clay	2	17.96	0.15	18.37
	Temperature, moisture, pH, NO_3-N, NH_4-N, DOC, TDN, SOC, SN, CN, clay	2	17.97	0.15	18.38
	Temperature, moisture, pH, NO_3-N, NH_4-N, TDN, SOC, SN, CN, clay	2	17.97	0.16	18.38
	Temperature, moisture, pH, NO_3-N, NH_4-N, SOC, SN, CN, clay	2	17.97	0.15	18.36
	Temperature, moisture, pH, NH_4-N, SOC, SN, CN, clay	2	17.97	0.16	18.36
	Temperature, moisture, pH, NH_4-N, SOC, CN, clay	2	18.01	0.19	18.38
	Temperature, moisture, NH_4-N, SOC, CN, clay	2	18.00	0.19	18.37
	Moisture, NH_4-N, SOC, CN, clay	2	17.99	0.18	18.35
	Moisture, NH_4-N, CN, clay	2	18.02	0.22	18.37
	Moisture, NH_4-N, clay	2	17.98	0.21	18.32
	Moisture, clay	2	17.92	0.22	18.28
	Moisture	2	17.96	0.22	18.30
Combined	Elevation, slope, aspect, TWI, TPI, NDVI, GNDVI, NDMI, temperature, moisture, pH, bulk density, NO_3-N, NH_4-N, DOC, TDN, SOC, SN, CN, sand, silt, clay	2	17.97	0.14	18.36
	Elevation, slope, aspect, TWI, NDVI, GNDVI, NDMI, temperature, moisture, pH, bulk density, NO_3-N, NH_4-N, DOC, TDN, SOC, SN, CN, sand, silt, clay	2	17.97	0.16	18.37
	Elevation, aspect, TWI, NDVI, GNDVI, NDMI, temperature, moisture, pH, bulk density, NO_3-N, NH_4-N, DOC, TDN, SOC, SN, CN, sand, silt, clay	2	17.97	0.16	18.37
	Elevation, aspect, NDVI, GNDVI, NDMI, temperature, moisture, pH, bulk density, NO_3-N, NH_4-N, DOC, TDN, SOC, SN, CN, sand, silt, clay	2	17.97	0.15	18.37
	Elevation, aspect, NDVI, GNDVI, NDMI, temperature, moisture, pH, NO_3-N, NH_4-N, DOC, TDN, SOC, SN, CN, sand, silt, clay	2	17.97	0.15	18.37
	Elevation, NDVI, GNDVI, NDMI, temperature, moisture, pH, NO_3-N, NH_4-N, DOC, TDN, SOC, SN, CN, sand, silt, clay	2	17.97	0.16	18.37
	Elevation, NDVI, GNDVI, NDMI, temperature, moisture, pH, NO_3-N, NH_4-N, DOC, TDN, SOC, SN, CN, silt, clay	2	17.98	0.17	18.39
	Elevation, NDVI, GNDVI, NDMI, temperature, moisture, pH, NO_3-N, NH_4-N, DOC, TDN, SOC, SN, CN, clay	2	18.00	0.19	18.40
	NDVI, GNDVI, NDMI, temperature, moisture, pH, NO_3-N, NH_4-N, DOC, TDN, SOC, SN, CN, clay	2	17.99	0.17	18.39
	NDVI, GNDVI, NDMI, temperature, moisture, pH, NO_3-N, NH_4-N, TDN, SOC, SN, CN, clay	2	17.98	0.17	18.38
	NDVI, GNDVI, NDMI, temperature, moisture, pH, NH_4-N, TDN, SOC, SN, CN, clay	2	17.99	0.18	18.39
	NDVI, GNDVI, NDMI, temperature, moisture, pH, NH_4-N, SOC, SN, CN, clay	2	17.99	0.19	18.38
	NDVI, GNDVI, NDMI, temperature, moisture, NH_4-N, SOC, SN, CN, clay	2	17.98	0.18	18.37
	NDVI, GNDVI, NDMI, moisture, NH_4-N, SOC, SN, CN, clay	2	17.99	0.19	18.38
	NDVI, GNDVI, NDMI, moisture, NH_4-N, SOC, CN, clay	2	18.01	0.20	18.38
	NDVI, GNDVI, NDMI, moisture, SOC, CN, clay	2	18.01	0.20	18.38
	NDVI, NDMI, moisture, SOC, CN, clay	2	18.02	0.21	18.38
	NDVI, NDMI, moisture, CN, clay	2	18.03	0.23	18.38
	NDVI, moisture, CN, clay	3	18.05	0.26	18.38
	NDVI, moisture, clay	2	17.98	0.24	18.32
	NDVI, moisture	2	18.05	0.25	18.37
	NDVI	2	17.81	0.11	18.16

B3c): Arable N_2O-N (positive & negative) flux

Category	Predictor variables	10-fold cross validation			
		mtry	RMSE	R^2	MAE
Remote sensing	Elevation, slope, aspect, TWI, TPI, NDVI, GNDVI, NDMI	5	18.37	0.56	18.53
	Elevation, slope, aspect, TWI, NDVI, GNDVI, NDMI	2	18.38	0.58	18.54
	Elevation, aspect, TWI, NDVI, GNDVI, NDMI	2	18.39	0.58	18.55
	Elevation, aspect, NDVI, GNDVI, NDMI	2	18.38	0.58	18.54
	Elevation, NDVI, GNDVI, NDMI	4	18.37	0.57	18.53
	Elevation, GNDVI, NDMI	2	18.36	0.57	18.53
	GNDVI, NDMI	2	18.32	0.53	18.50
	GNDVI	2	18.21	0.45	18.42
Site measured soil parameters	Tmperature, moisture, pH, bulk density, NO_3-N, NH_4-N, DOC, TDN, SOC, SN, CN, sand, silt, clay	8	18.27	0.44	18.45
	Temperature, moisture, pH, NO_3-N, NH_4-N, DOC, TDN, SOC, SN, CN, sand, silt, clay	13	18.28	0.46	18.46
	Temperature, moisture, pH, NO_3-N, NH_4-N, DOC, SOC, SN, CN, sand, silt, clay	12	18.29	0.46	18.46
	Moisture, pH, NO_3-N, NH_4-N, DOC, SOC, SN, CN, sand, silt, clay	11	18.30	0.48	18.47
	Moisture, pH, NO_3-N, NH_4-N, DOC, SOC, SN, CN, sand, silt	10	18.29	0.47	18.47
	Moisture, pH, NO_3-N, DOC, SOC, SN, CN, sand, silt	9	18.29	0.47	18.47
	Moisture, NO_3-N, DOC, SOC, SN, CN, sand, silt	8	18.29	0.46	18.46
	Moisture, NO_3-N, SOC, SN, CN, sand, silt	7	18.29	0.47	18.46
	Moisture, NO_3-N, SN, CN, sand, silt	6	18.30	0.48	18.47
	Moisture, NO_3-N, SN, CN, sand	2	18.29	0.47	18.47
	Moisture, NO_3-N, SN, CN	2	18.28	0.46	18.48
	Moisture, SN, CN	2	18.22	0.41	18.43
	Moisture, SN	2	18.22	0.41	18.43
	Moisture	2	18.12	0.33	18.34
Combined	Elevation, slope, aspect, TWI, TPI, NDVI, GNDVI, NDMI, temperature, moisture, pH, bulk density, NO_3-N, NH_4-N, DOC, TDN, SOC, SN, CN, sand, silt, clay	12	18.39	0.57	18.55
	Elevation, aspect, TWI, TPI, NDVI, GNDVI, NDMI, temperature, moisture, pH, bulk density, NO_3-N, NH_4-N, DOC, TDN, SOC, SN, CN, sand, silt, clay	11	18.38	0.57	18.55
	Elevation, aspect, TWI, TPI, NDVI, GNDVI, NDMI, temperature, moisture, pH, bulk density, NO_3-N, NH_4-N, DOC, TDN, SOC, SN, CN, sand, silt	11	18.38	0.57	18.54
	Elevation, aspect, TWI, NDVI, GNDVI, NDMI, temperature, moisture, pH, bulk density, NO_3-N, NH_4-N, DOC, TDN, SOC, SN, CN, sand, silt	10	18.38	0.57	18.55
	Elevation, aspect, NDVI, GNDVI, NDMI, temperature, moisture, pH, bulk density, NO_3-N, NH_4-N, DOC, TDN, SOC, SN, CN, sand, silt	10	18.38	0.57	18.54
	Elevation, aspect, NDVI, GNDVI, NDMI, temperature, moisture, pH, NO_3-N, NH_4-N, DOC, TDN, SOC, SN, CN, sand, silt	9	18.38	0.57	18.54
	Elevation, aspect, NDVI, GNDVI, NDMI, temperature, moisture, pH, NO_3-N, NH_4-N, DOC, TDN, SOC, SN, CN, silt	9	18.38	0.57	18.54
	Elevation, aspect, NDVI, GNDVI, NDMI, temperature, moisture, pH, NO_3-N, NH_4-N, DOC, TDN, SOC, SN, CN	2	18.37	0.57	18.54
	Elevation, NDVI, GNDVI, NDMI, temperature, moisture, pH, NO_3-N, NH_4-N, DOC, TDN, SOC, SN, CN	8	18.38	0.57	18.54
	Elevation, NDVI, GNDVI, NDMI, moisture, pH, NO_3-N, NH_4-N, DOC, TDN, SOC, SN, CN	7	18.38	0.57	18.54
	NDVI, GNDVI, NDMI, moisture, pH, NO_3-N, NH_4-N, DOC, TDN, SOC, SN, CN	7	18.38	0.57	18.54
	NDVI, GNDVI, NDMI, moisture, NO_3-N, NH_4-N, DOC, TDN, SOC, SN, CN	6	18.38	0.57	18.54
	NDVI, GNDVI, NDMI, moisture, NO_3-N, DOC, TDN, SOC, SN, CN	6	18.37	0.56	18.54
	NDVI, GNDVI, NDMI, moisture, NO_3-N, TDN, SOC, SN, CN	2	18.38	0.57	18.54
	NDVI, GNDVI, NDMI, moisture, TDN, SOC, SN, CN	2	18.37	0.56	18.54
	NDVI, GNDVI, NDMI, moisture, TDN, SOC, SN	2	18.37	0.55	18.53
	NDVI, GNDVI, NDMI, moisture, TDN, SN	2	18.38	0.57	18.54
	NDVI, GNDVI, NDMI, moisture, SN	2	18.35	0.54	18.51
	NDVI, GNDVI, NDMI, moisture	2	18.36	0.56	18.52
	GNDVI, NDMI, moisture	2	18.32	0.52	18.49
	GNDVI, NDMI	2	18.32	0.53	18.50
	GNDVI	2	18.21	0.45	18.42

Table B4 a, b, c: Cross-validation results of different models developed for negative CH_4 fluxes in 4a) forest, 4b) grassland and 4c) arable land using different predictors in the training dataset. Stepwise elimination of least important predictors was implemented.

B4a): Forest CH_4-C negative fluxes only — **10-fold cross validation**

Category	Predictor variables	mtry	RMSE	R^2	MAE
Remote sensing	Elevation, slope, aspect, TWI, TPI, NDVI, GNDVI, NDMI	8	39.38	0.21	32.51
	Elevation, slope, aspect, TPI, NDVI, GNDVI, NDMI	2	39.45	0.20	32.64
	Elevation, aspect, TPI, NDVI, GNDVI, NDMI	2	39.11	0.20	32.45
	Elevation, aspect, NDVI, GNDVI, NDMI	5	39.53	0.20	32.43
	Elevation, aspect, NDVI, NDMI	4	39.76	0.20	32.57
	Elevation, aspect, NDVI	3	40.42	0.19	32.69
	Aspect, NDVI	2	41.52	0.17	33.61
	Aspect	2	46.08	0.09	35.89
Site measured soil parameters	Temperature, moisture, pH, bulk density, NO_3-N, NH_4-N, DOC, TDN, SOC, SN, CN, sand, silt, clay	2	40.59	0.14	32.82
	Temperature, moisture, pH, bulk density, NO_3-N, NH_4-N, DOC, TDN, SOC, SN, sand, silt, clay	2	40.17	0.16	32.57
	Temperature, moisture, pH, NO_3-N, NH_4-N, DOC, TDN, SOC, SN, sand, silt, clay	2	40.09	0.17	32.52
	Moisture, pH, NO_3-N, NH_4-N, DOC, TDN, SOC, SN, sand, silt, clay	2	40.16	0.16	32.68
	Moisture, pH, NO_3-N, NH_4-N, DOC, TDN, SOC, SN, sand, silt	2	40.22	0.16	32.65
	Moisture, pH, NO_3-N, NH_4-N, DOC, TDN, SOC, SN, sand	5	40.66	0.16	32.59
	Moisture, pH, NO_3-N, NH_4-N, DOC, SOC, SN, sand	2	40.33	0.16	32.35
	Moisture, pH, NO_3-N, DOC, SOC, SN, sand	2	40.02	0.17	32.19
	Moisture, pH, NO_3-N, SOC, SN, sand	2	40.21	0.17	32.05
	Moisture, pH, NO_3-N, SOC, sand	2	40.01	0.18	31.78
	Moisture, pH, NO_3-N, SOC	2	41.27	0.14	32.39
	Moisture, pH, NO_3-N	2	41.67	0.15	32.38
	pH, NO_3-N	2	43.94	0.12	34.03
	NO_3-N	2	47.96	0.10	37.11
Combined	Elevation, slope, aspect, TWI, TPI, NDVI, GNDVI, NDMI, temperature, moisture, pH, bulk density, NO_3-N, NH_4-N, DOC, TDN, SOC, SN, CN, sand, silt, clay	12	39.66	0.19	32.09
	Elevation, aspect, TWI, TPI, NDVI, GNDVI, NDMI, temperature, moisture, pH, bulk density, NO_3-N, NH_4-N, DOC, TDN, SOC, SN, CN, sand, silt, clay	11	39.59	0.20	32.09
	Elevation, aspect, TWI, TPI, NDVI, GNDVI, NDMI, temperature, moisture, pH, bulk density, NO_3-N, NH_4-N, DOC, TDN, SOC, SN, sand, silt, clay	20	39.49	0.20	31.90
	Elevation, aspect, TPI, NDVI, GNDVI, NDMI, temperature, moisture, pH, bulk density, NO_3-N, NH_4-N, DOC, TDN, SOC, SN, sand, silt, clay	10	39.17	0.21	31.82
	Elevation, aspect, TPI, NDVI, GNDVI, temperature, moisture, pH, bulk density, NO_3-N, NH_4-N, DOC, TDN, SOC, SN, sand, silt, clay	10	39.11	0.21	31.73
	Elevation, aspect, TPI, NDVI, GNDVI, temperature, moisture, pH, NO_3-N, NH_4-N, DOC, TDN, SOC, SN, sand, silt, clay	9	38.95	0.22	31.61
	Elevation, aspect, TPI, NDVI, GNDVI, temperature, moisture, pH, NO_3-N, NH_4-N, DOC, SOC, SN, sand, silt, clay	9	38.79	0.23	31.43
	Elevation, aspect, NDVI, GNDVI, temperature, moisture, pH, NO_3-N, NH_4-N, DOC, SOC, SN, sand, silt, clay	8	38.73	0.23	31.44
	Elevation, aspect, NDVI, GNDVI, temperature, moisture, pH, NO_3-N, DOC, SOC, SN, sand, silt, clay	8	38.48	0.24	31.20
	Elevation, aspect, NDVI, GNDVI, temperature, moisture, pH, NO_3-N, DOC, SOC, SN, sand, silt	7	38.35	0.24	31.11
	Elevation, aspect, NDVI, GNDVI, temperature, moisture, pH, NO_3-N, SOC, SN, sand, silt	2	37.86	0.26	30.79
	Aspect, NDVI, GNDVI, temperature, moisture, pH, NO_3-N, SOC, SN, sand, silt	2	37.55	0.28	30.57
	Aspect, NDVI, GNDVI, temperature, moisture, pH, NO_3-N, SOC, SN, silt	2	37.75	0.27	30.72
	Aspect, NDVI, GNDVI, moisture, pH, NO_3-N, SOC, SN, silt	2	37.96	0.25	31.07
	Aspect, NDVI, GNDVI, moisture, pH, NO_3-N, SOC, SN	2	38.00	0.25	31.04
	Aspect, NDVI, GNDVI, moisture, pH, NO_3-N, SOC	2	37.88	0.25	30.83
	Aspect, NDVI, moisture, pH, NO_3-N, SOC	2	37.98	0.25	30.87
	Aspect, moisture, pH, NO_3-N, SOC	2	38.83	0.22	31.24
	Aspect, moisture, pH, NO_3-N	2	38.25	0.25	30.70
	Aspect, pH, NO_3-N	2	39.96	0.21	31.88
	Aspect, NO_3-N	2	41.25	0.19	32.84
	Aspect	2	46.08	0.09	35.89

B4b): Grassland CH_4-C negative fluxes only

Category	Predictor variables	10-fold cross validation: mtry	RMSE	R^2	MAE
Remote sensing	Elevation, slope, aspect, TWI, TPI, NDVI, GNDVI, NDMI	2	17.33	0.15	13.63
	Elevation, slope, aspect, TPI, NDVI, GNDVI, NDMI	2	17.23	0.15	13.58
	Elevation, aspect, TPI, NDVI, GNDVI, NDMI	2	17.28	0.14	13.70
	Elevation, TPI, NDVI, GNDVI, NDMI	2	16.93	0.17	13.53
	Elevation, NDVI, GNDVI, NDMI	2	17.00	0.16	13.71
	NDVI, GNDVI, NDMI	2	17.14	0.16	13.63
	NDVI, NDMI	2	17.66	0.15	14.11
	NDMI	2	17.72	0.18	13.86
Site measured soil parameters	Temperature, moisture, pH, bulk density, NO_3-N, NH_4-N, DOC, TDN, SOC, SN, CN, sand, silt, clay	2	15.86	0.25	12.37
	Temperature, moisture, pH, bulk density, NO_3-N, DOC, TDN, SOC, SN, CN, sand, silt, clay	2	15.70	0.27	12.21
	Moisture, pH, bulk density, NO_3-N, DOC, TDN, SOC, SN, CN, sand, silt, clay	2	15.50	0.29	12.07
	Moisture, pH, bulk density, NO_3-N, DOC, TDN, SN, CN, sand, silt, clay	2	15.47	0.29	12.04
	Moisture, pH, bulk density, NO_3-N, DOC, SN, CN, sand, silt, clay	2	15.35	0.31	11.95
	Moisture, pH, bulk density, DOC, SN, CN, sand, silt, clay	2	15.39	0.30	12.00
	Moisture, pH, bulk density, DOC, CN, sand, silt, clay	2	15.29	0.31	11.94
	Moisture, pH, DOC, CN, sand, silt, clay	2	15.36	0.30	12.05
	Moisture, pH, DOC, CN, silt, clay	2	15.40	0.30	12.01
	Moisture, pH, CN, silt, clay	2	15.14	0.33	11.79
	Moisture, pH, CN, clay	2	15.32	0.33	11.77
	pH, CN, clay	2	15.61	0.33	11.69
	pH, clay	2	15.80	0.33	11.84
	pH	2	18.06	0.20	14.43
Combined	Elevation, slope, aspect, TWI, TPI, NDVI, GNDVI, NDMI, temperature, moisture, pH, bulk density, NO_3-N, NH_4-N, DOC, TDN, SOC, SN, CN, sand, silt, clay	12	15.70	0.26	12.22
	Elevation, slope, aspect, TWI, TPI, NDVI, GNDVI, NDMI, temperature, moisture, pH, bulk density, NO_3-N, NH_4-N, DOC, TDN, SN, CN, sand, silt, clay	11	15.61	0.27	12.12
	Elevation, slope, aspect, TWI, TPI, NDVI, NDMI, temperature, moisture, pH, bulk density, NO_3-N, NH_4-N, DOC, TDN, SN, CN, sand, silt, clay	11	15.60	0.27	12.12
	Elevation, slope, aspect, TPI, NDVI, NDMI, temperature, moisture, pH, bulk density, NO_3-N, NH_4-N, DOC, TDN, SN, CN, sand, silt, clay	10	15.56	0.28	12.08
	Elevation, slope, aspect, TPI, NDVI, NDMI, temperature, moisture, pH, bulk density, NO_3-N, NH_4-N, DOC, TDN, SN, CN, silt, clay	10	15.52	0.28	12.03
	Elevation, aspect, TPI, NDVI, NDMI, temperature, moisture, pH, bulk density, NO_3-N, NH_4-N, DOC, TDN, SN, CN, silt, clay	9	15.54	0.27	12.10
	Elevation, aspect, TPI, NDVI, NDMI, temperature, moisture, pH, bulk density, NH_4-N, DOC, TDN, SN, CN, silt, clay	9	15.54	0.28	12.07
	Elevation, aspect, TPI, NDVI, NDMI, temperature, moisture, pH, bulk density, DOC, TDN, SN, CN, silt, clay	8	15.37	0.29	11.93
	Elevation, aspect, TPI, NDVI, NDMI, temperature, moisture, pH, bulk density, DOC, TDN, CN, silt, clay	8	15.41	0.29	11.94
	Elevation, TPI, NDVI, NDMI, temperature, moisture, pH, bulk density, DOC, TDN, CN, silt, clay	2	15.16	0.30	11.87
	Elevation, TPI, NDVI, NDMI, moisture, pH, bulk density, DOC, TDN, CN, silt, clay	2	14.98	0.32	11.73
	Elevation, NDVI, NDMI, moisture, pH, bulk density, DOC, TDN, CN, silt, clay	2	15.18	0.29	12.00
	Elevation, NDVI, NDMI, moisture, pH, DOC, TDN, CN, silt, clay	2	15.16	0.29	11.98
	Elevation, NDVI, NDMI, moisture, pH, DOC, CN, silt, clay	2	15.17	0.30	11.98
	Elevation, NDMI, moisture, pH, DOC, CN, silt, clay	2	15.06	0.31	11.76
	NDMI, moisture, pH, DOC, CN, silt, clay	2	15.17	0.31	11.83
	NDMI, moisture, pH, CN, silt, clay	2	14.84	0.34	11.54
	NDMI, moisture, pH, CN, clay	2	14.87	0.34	11.43
	Moisture, pH, CN, clay	2	15.32	0.33	11.77
	pH, CN, clay	2	15.61	0.33	11.69
	pH, clay	2	15.80	0.33	11.84
	pH	2	18.06	0.20	14.43

B4c): Arable CH_4-C negatives flux only

Category	Predictor variables	mtry	RMSE	R^2	MAE
		10-fold cross validation			
Remote sensing	Elevation, slope, aspect, TWI, TPI, NDVI, GNDVI, NDMI	2	19.54	0.42	14.72
	Elevation, slope, aspect, TWI, NDVI, GNDVI, NDMI	2	19.05	0.44	14.22
	Elevation, slope, aspect, NDVI, GNDVI, NDMI	2	18.72	0.47	13.86
	Elevation, aspect, NDVI, GNDVI, NDMI	2	18.88	0.46	13.89
	Elevation, NDVI, GNDVI, NDMI	2	19.47	0.39	14.92
	Elevation, NDVI, GNDVI	2	19.20	0.40	14.81
	Elevation, GNDVI	2	20.71	0.36	15.66
	GNDVI	2	17.66	0.48	13.16
Site measured soil parameters	Temperature, moisture, pH, bulk density, NO_3-N, NH_4-N, DOC, TDN, SOC, SN, CN, sand, silt, clay	2	17.48	0.50	13.27
	Moisture, pH, bulk density, NO_3-N, NH_4-N, DOC, TDN, SOC, SN, CN, sand, silt, clay	2	17.27	0.52	13.03
	Moisture, pH, bulk density, NO_3-N, NH_4-N, DOC, TDN, SOC, SN, CN, sand, clay	2	17.26	0.52	13.01
	Moisture, pH, bulk density, NO_3-N, NH_4-N, DOC, TDN, SOC, SN, CN, clay	2	17.37	0.52	13.01
	Moisture, pH, bulk density, NH_4-N, DOC, TDN, SOC, SN, CN, clay	2	17.38	0.51	12.96
	Moisture, pH, bulk density, NH_4-N, DOC, SOC, SN, CN, clay	2	17.65	0.50	13.16
	Moisture, pH, NH_4-N, DOC, SOC, SN, CN, clay	2	17.55	0.51	12.92
	Moisture, pH, NH_4-N, DOC, SOC, SN, CN	2	17.67	0.49	13.17
	Moisture, pH, NH_4-N, DOC, SN, CN	2	17.94	0.47	13.27
	Moisture, pH, DOC, SN, CN	2	18.01	0.48	13.29
	Moisture, pH, SN, CN	2	17.77	0.50	13.11
	Moisture, pH, CN	2	17.70	0.50	13.20
	Moisture, CN	2	17.20	0.56	12.84
	CN	2	18.35	0.47	13.70
Combined	Elevation, slope, aspect, TWI, TPI, NDVI, GNDVI, NDMI, temperature, moisture, pH, bulk density, NO_3-N, NH_4-N, DOC, TDN, SOC, SN, CN, sand, silt, clay	22	18.01	0.51	13.33
	Elevation, aspect, TWI, TPI, NDVI, GNDVI, NDMI, temperature, moisture, pH, bulk density, NO_3-N, NH_4-N, DOC, TDN, SOC, SN, CN, sand, silt, clay	21	17.96	0.51	13.26
	Elevation, aspect, TWI, TPI, NDVI, GNDVI, NDMI, temperature, moisture, pH, bulk density, NO_3-N, NH_4-N, DOC, TDN, SOC, SN, CN, sand, clay	20	18.02	0.51	13.29
	Elevation, aspect, TWI, TPI, NDVI, GNDVI, NDMI, moisture, pH, bulk density, NO_3-N, NH_4-N, DOC, TDN, SOC, SN, CN, sand, clay	19	17.92	0.51	13.20
	Elevation, aspect, TPI, NDVI, GNDVI, NDMI, moisture, pH, bulk density, NO_3-N, NH_4-N, DOC, TDN, SOC, SN, CN, sand, clay	18	17.80	0.52	13.14
	Elevation, aspect, NDVI, GNDVI, NDMI, moisture, pH, bulk density, NO_3-N, NH_4-N, DOC, TDN, SOC, SN, CN, sand, clay	17	17.77	0.52	13.15
	Elevation, aspect, NDVI, GNDVI, NDMI, moisture, pH, NO_3-N, NH_4-N, DOC, TDN, SOC, SN, CN, sand, clay	2	17.48	0.51	13.04
	Elevation, aspect, NDVI, GNDVI, NDMI, moisture, pH, NO_3-N, NH_4-N, DOC, TDN, SOC, SN, CN, clay	2	17.66	0.51	13.11
	Elevation, aspect, NDVI, GNDVI, NDMI, moisture, pH, NO_3-N, NH_4-N, DOC, TDN, SN, CN, clay	2	17.60	0.51	13.04
	Elevation, aspect, NDVI, GNDVI, NDMI, moisture, pH, NH_4-N, DOC, TDN, SN, CN, clay	2	17.57	0.52	13.04
	Elevation, aspect, NDVI, GNDVI, NDMI, moisture, pH, NH_4-N, DOC, SN, CN, clay	2	17.85	0.50	13.25
	Elevation, aspect, NDVI, GNDVI, NDMI, moisture, pH, DOC, SN, CN, clay	2	17.73	0.51	13.12
	Elevation, aspect, NDVI, GNDVI, NDMI, moisture, pH, DOC, SN, CN	2	17.71	0.51	13.27
	Elevation, NDVI, GNDVI, NDMI, moisture, pH, DOC, SN, CN	2	18.25	0.47	14.02
	Elevation, NDVI, GNDVI, NDMI, moisture, pH, DOC, CN	2	18.26	0.46	14.10
	Elevation, GNDVI, NDMI, moisture, pH, DOC, CN	2	18.45	0.47	14.12
	Elevation, GNDVI, NDMI, moisture, pH, CN	2	18.36	0.47	14.13
	Elevation, GNDVI, moisture, pH, CN	2	18.12	0.48	13.93
	GNDVI, moisture, pH, CN	2	17.79	0.49	13.49
	Moisture, pH, CN	2	17.70	0.50	13.20
	Moisture, CN	2	17.20	0.56	12.84
	CN	2	18.35	0.47	13.70

Table B5 a, b, c: Cross-validation results of different models developed for positive N_2O fluxes in 5a) forest, 5b) grassland and 5c) arable land using different predictors in the training dataset. Stepwise elimination of least important predictors was implemented.

B5a): Forest N_2O-N positive fluxes only		**10-fold cross validation**			
Category	**Predictor variables**	**mtry**	**RMSE**	**R^2**	**MAE**
Remote sensing	Elevation, slope, aspect, TWI, TPI, NDVI, GNDVI, NDMI	2	18.60	0.15	18.73
	Elevation, aspect, TWI, TPI, NDVI, GNDVI, NDMI	2	18.60	0.15	18.73
	Elevation, aspect, TPI, NDVI, GNDVI, NDMI	2	18.61	0.17	18.74
	Elevation, aspect, NDVI, GNDVI, NDMI	2	18.61	0.19	18.74
	Aspect, NDVI, GNDVI, NDMI	2	18.61	0.23	18.74
	Aspect, NDVI, NDMI	2	18.60	0.19	18.73
	Aspect, NDVI	2	18.61	0.26	18.74
	NDVI	2	18.57	0.19	18.72
Site measured soil parameters	Temperature, moisture, pH, bulk density, NO_3-N, NH_4-N, DOC, TDN, SOC, SN, CN, sand, silt, clay	14	18.63	0.24	18.75
	Temperature, moisture, pH, bulk density, NO_3-N, DOC, TDN, SOC, SN, CN, sand, silt, clay	13	18.63	0.23	18.75
	Temperature, moisture, bulk density, NO_3-N, DOC, TDN, SOC, SN, CN, sand, silt, clay	12	18.64	0.24	18.75
	Temperature, moisture, bulk density, NO_3-N, DOC, TDN, SOC, CN, sand, silt, clay	11	18.64	0.25	18.75
	Temperature, moisture, bulk density, NO_3-N, DOC, TDN, SOC, sand, silt, clay	10	18.64	0.25	18.75
	Temperature, moisture, bulk density, NO_3-N, DOC, TDN, sand, silt, clay	9	18.64	0.25	18.75
	Temperature, moisture, bulk density, NO_3-N, DOC, sand, silt, clay	8	18.64	0.25	18.75
	Temperature, moisture, bulk density, NO_3-N, DOC, silt, clay	7	18.65	0.26	18.76
	Temperature, moisture, bulk density, NO_3-N, silt, clay	6	18.64	0.26	18.75
	Moisture, bulk density, NO_3-N, silt, clay	2	18.64	0.27	18.75
	Moisture, bulk density, silt, clay	2	18.62	0.20	18.74
	Moisture, silt, clay	2	18.61	0.19	18.73
	Silt, clay	2	18.58	0.17	18.71
	Silt	2	18.57	0.16	18.70
Combined	Elevation, slope, aspect, TWI, TPI, NDVI, GNDVI, NDMI, temperature, moisture, pH, bulk density, NO_3-N, NH_4-N, DOC, TDN, SOC, SN, CN, sand, silt, clay	22	18.64	0.25	18.76
	Elevation, slope, aspect, TWI, TPI, GNDVI, NDMI, temperature, moisture, pH, bulk density, NO_3-N, NH_4-N, DOC, TDN, SOC, SN, CN, sand, silt, clay	21	18.65	0.25	18.76
	Elevation, slope, aspect, TPI, GNDVI, NDMI, temperature, moisture, pH, bulk density, NO_3-N, NH_4-N, DOC, TDN, SOC, SN, CN, sand, silt, clay	20	18.64	0.25	18.76
	Elevation, slope, aspect, GNDVI, NDMI, temperature, moisture, pH, bulk density, NO_3-N, NH_4-N, DOC, TDN, SOC, SN, CN, sand, silt, clay	19	18.64	0.25	18.76
	Elevation, aspect, GNDVI, NDMI, temperature, moisture, pH, bulk density, NO_3-N, NH_4-N, DOC, TDN, SOC, SN, CN, sand, silt, clay	18	18.65	0.25	18.76
	Elevation, aspect, GNDVI, NDMI, temperature, moisture, pH, bulk density, NO_3-N, DOC, TDN, SOC, SN, CN, sand, silt, clay	17	18.64	0.25	18.76
	Elevation, aspect, GNDVI, NDMI, temperature, moisture, pH, bulk density, NO_3-N, DOC, TDN, SOC, CN, sand, silt, clay	16	18.65	0.26	18.76
	Aspect, GNDVI, NDMI, temperature, moisture, pH, bulk density, NO_3-N, DOC, TDN, SOC, CN, sand, silt, clay	15	18.65	0.26	18.76
	Aspect, GNDVI, NDMI, temperature, moisture, bulk density, NO_3-N, DOC, TDN, SOC, CN, sand, silt, clay	14	18.65	0.26	18.76
	Aspect, GNDVI, NDMI, temperature, moisture, bulk density, NO_3-N, DOC, TDN, SOC, sand, silt, clay	2	18.65	0.28	18.76
	Aspect, GNDVI, NDMI, temperature, moisture, bulk density, NO_3-N, DOC, TDN, sand, silt, clay	2	18.65	0.28	18.76
	Aspect, NDMI, temperature, moisture, bulk density, NO_3-N, DOC, TDN, sand, silt, clay	2	18.65	0.26	18.76
	Aspect, NDMI, temperature, moisture, bulk density, NO_3-N, DOC, sand, silt, clay	2	18.65	0.25	18.76
	Aspect, temperature, moisture, bulk density, NO_3-N, DOC, sand, silt, clay	5	18.65	0.25	18.75
	Aspect, temperature, moisture, bulk density, NO_3-N, DOC, silt, clay	2	18.65	0.26	18.76
	Aspect, temperature, moisture, bulk density, DOC, silt, clay	7	18.65	0.25	18.76
	Aspect, temperature, moisture, DOC, silt, clay	6	18.66	0.26	18.76
	Aspect, temperature, moisture, DOC, silt	5	18.67	0.29	18.77
	Aspect, temperature, moisture, silt	3	18.66	0.26	18.76
	Aspect, moisture, silt	2	18.65	0.27	18.76
	Moisture, silt	2	18.62	0.22	18.74
	Silt	2	18.57	0.16	18.70

B5b): Grassland N_2O-N positive fluxes only		**10-fold cross validation**			
Category	**Predictor variables**	**mtry**	**RMSE**	**R^2**	**MAE**
Remote sensing	Elevation, slope, aspect, TWI, TPI, NDVI, GNDVI, NDMI	2	18.35	0.26	18.54
	Elevation, slope, aspect, TPI, NDVI, GNDVI, NDMI	4	18.33	0.26	18.53
	Elevation, slope, aspect, NDVI, GNDVI, NDMI	4	18.34	0.27	18.54
	Elevation, slope, aspect, NDVI, NDMI	2	18.35	0.27	18.55
	Elevation, aspect, NDVI, NDMI	4	18.34	0.25	18.54
	Elevation, NDVI, NDMI	3	18.35	0.25	18.56
	Elevation, NDMI	2	18.37	0.28	18.55
	Elevation	2	18.37	0.35	18.55
Site measured soil parameters	Temperature, moisture, pH, bulk density, NO_3-N, NH_4-N, DOC, TDN, SOC, SN, CN, sand, silt, clay	2	18.34	0.18	18.54
	Temperature, moisture, pH, bulk density, NO_3-N, NH_4-N, TDN, SOC, SN, CN, sand, silt, clay	2	18.34	0.19	18.54
	Temperature, moisture, pH, NO_3-N, NH_4-N, TDN, SOC, SN, CN, sand, silt, clay	2	18.35	0.19	18.55
	Temperature, moisture, pH, NO_3-N, NH_4-N, TDN, SOC, SN, CN, silt, clay	2	18.35	0.20	18.55
	Moisture, pH, NO_3-N, NH_4-N, TDN, SOC, SN, CN, silt, clay	2	18.34	0.19	18.54
	Moisture, pH, NO_3-N, NH_4-N, TDN, SOC, SN, CN, clay	2	18.35	0.22	18.54
	Moisture, pH, NO_3-N, NH_4-N, TDN, SN, CN, clay	2	18.36	0.22	18.55
	Moisture, pH, NH_4-N, TDN, SN, CN, clay	2	18.36	0.23	18.55
	Moisture, NH_4-N, TDN, SN, CN, clay	2	18.37	0.25	18.55
	Moisture, NH_4-N, TDN, CN, clay	2	18.37	0.26	18.56
	Moisture, TDN, CN, clay	2	18.40	0.33	18.58
	Moisture, TDN, clay	2	18.43	0.37	18.60
	Moisture, clay	2	18.36	0.31	18.57
	Moisture	2	18.34	0.25	18.58
Combined	Elevation, slope, aspect, TWI, TPI, NDVI, GNDVI, NDMI, temperature, moisture, pH, bulk density, NO_3-N, NH_4-N, DOC, TDN, SOC, SN, CN, sand, silt, clay	2	18.36	0.21	18.55
	Elevation, slope, aspect, TWI, TPI, NDVI, GNDVI, NDMI, temperature, moisture, pH, bulk density, NO_3-N, NH_4-N, TDN, SOC, SN, CN, sand, silt, clay	2	18.36	0.22	18.55
	Elevation, slope, aspect, TWI, TPI, NDVI, GNDVI, NDMI, temperature, moisture, pH, NO_3-N, NH_4-N, TDN, SOC, SN, CN, sand, silt, clay	2	18.37	0.23	18.56
	Elevation, slope, aspect, TPI, NDVI, GNDVI, NDMI, temperature, moisture, pH, NO_3-N, NH_4-N, TDN, SOC, SN, CN, sand, silt, clay	2	18.36	0.23	18.55
	Elevation, slope, aspect, TPI, NDVI, NDMI, temperature, moisture, pH, NO_3-N, NH_4-N, TDN, SOC, SN, CN, sand, silt, clay	2	18.37	0.24	18.55
	Elevation, slope, aspect, NDVI, NDMI, temperature, moisture, pH, NO_3-N, NH_4-N, TDN, SOC, SN, CN, sand, silt, clay	2	18.37	0.23	18.56
	Elevation, aspect, NDVI, NDMI, temperature, moisture, pH, NO_3-N, NH_4-N, TDN, SOC, SN, CN, sand, silt, clay	2	18.36	0.23	18.56
	Elevation, NDVI, NDMI, temperature, moisture, pH, NO_3-N, NH_4-N, TDN, SOC, SN, CN, sand, silt, clay	2	18.36	0.21	18.55
	Elevation, NDVI, NDMI, temperature, moisture, pH, NO_3-N, NH_4-N, TDN, SOC, SN, CN, silt, clay	2	18.36	0.22	18.56
	Elevation, NDVI, NDMI, temperature, moisture, pH, NO_3-N, NH_4-N, TDN, SOC, CN, silt, clay	2	18.37	0.23	18.56
	Elevation, NDVI, NDMI, temperature, moisture, NO_3-N, NH_4-N, TDN, SOC, CN, silt, clay	2	18.37	0.24	18.57
	Elevation, NDVI, NDMI, temperature, moisture, NO_3-N, NH_4-N, TDN, CN, silt, clay	2	18.38	0.24	18.58
	Elevation, NDVI, NDMI, moisture, NO_3-N, NH_4-N, TDN, CN, silt, clay	2	18.38	0.23	18.57
	Elevation, NDVI, NDMI, moisture, NH_4-N, TDN, CN, silt, clay	2	18.39	0.26	18.58
	Elevation, NDVI, NDMI, moisture, TDN, CN, silt, clay	2	18.40	0.28	18.58
	Elevation, NDVI, NDMI, moisture, TDN, CN, clay	2	18.41	0.31	18.59
	NDVI, NDMI, moisture, TDN, CN, clay	2	18.41	0.31	18.59
	NDMI, moisture, TDN, CN, clay	2	18.41	0.33	18.60
	NDMI, moisture, TDN, clay	2	18.44	0.37	18.61
	NDMI, moisture, TDN	2	18.42	0.31	18.61
	NDMI, moisture	2	18.47	0.38	18.63
	NDMI	2	18.22	0.11	18.47

B5c): Arable N_2O-N positive fluxes only

Category	Predictor variables	10-fold cross validation			
		mtry	**RMSE**	**R^2**	**MAE**
Remote sensing	Elevation, slope, aspect, TWI, TPI, NDVI, GNDVI, NDMI	5	18.47	0.63	18.59
	Elevation, aspect, TWI, TPI, NDVI, GNDVI, NDMI	4	18.48	0.64	18.60
	Elevation, aspect, TPI, NDVI, GNDVI, NDMI	4	18.49	0.65	18.61
	Elevation, aspect, NDVI, GNDVI, NDMI	2	18.50	0.66	18.62
	Elevation, NDVI, GNDVI, NDMI	2	18.48	0.65	18.61
	NDVI, GNDVI, NDMI	2	18.48	0.65	18.61
	GNDVI, NDMI	2	18.45	0.63	18.59
	GNDVI	2	18.31	0.51	18.51
Site measured soil parameters	Temperature, moisture, pH, bulk density, NO_3-N, NH_4-N, DOC, TDN, SOC, SN, CN, sand, silt, clay	2	18.26	0.39	18.42
	Temperature, moisture, pH, bulk density, NO_3-N, NH_4-N, DOC, TDN, SOC, SN, CN, silt, clay	2	18.27	0.40	18.43
	Temperature, moisture, pH, NO_3-N, NH_4-N, DOC, TDN, SOC, SN, CN, silt, clay	2	18.28	0.41	18.43
	Temperature, moisture, NO_3-N, NH_4-N, DOC, TDN, SOC, SN, CN, silt, clay	2	18.28	0.42	18.44
	Temperature, moisture, NO_3-N, NH_4-N, DOC, TDN, SOC, SN, CN, clay	2	18.28	0.42	18.44
	Moisture, NO_3-N, NH_4-N, DOC, TDN, SOC, SN, CN, clay	2	18.28	0.41	18.44
	Moisture, NO_3-N, NH_4-N, DOC, TDN, SOC, SN, CN	2	18.26	0.38	18.42
	Moisture, NO_3-N, NH_4-N, TDN, SOC, SN, CN	2	18.26	0.39	18.42
	Moisture, NO_3-N, NH_4-N, SOC, SN, CN	4	18.24	0.37	18.42
	Moisture, NO_3-N, NH_4-N, SN, CN	2	18.26	0.39	18.43
	Moisture, NO_3-N, NH_4-N, SN	2	18.27	0.40	18.43
	Moisture, NO_3-N, SN	2	18.25	0.38	18.42
	Moisture, SN	2	18.21	0.34	18.39
	Moisture	2	18.09	0.29	18.31
Combined	Elevation, slope, aspect, TWI, TPI, NDVI, GNDVI, NDMI, temperature, moisture, pH, bulk density, NO_3-N, NH_4-N, DOC, TDN, SOC, SN, CN, sand, silt, clay	12	18.46	0.62	18.60
	Elevation, slope, aspect, TPI, NDVI, GNDVI, NDMI, temperature, moisture, pH, bulk density, NO_3-N, NH_4-N, DOC, TDN, SOC, SN, CN, sand, silt, clay	11	18.46	0.62	18.60
	Elevation, slope, aspect, TPI, NDVI, GNDVI, NDMI, temperature, moisture, pH, bulk density, NO_3-N, NH_4-N, DOC, TDN, SOC, SN, CN, silt, clay	11	18.47	0.62	18.60
	Elevation, aspect, TPI, NDVI, GNDVI, NDMI, temperature, moisture, pH, bulk density, NO_3-N, NH_4-N, DOC, TDN, SOC, SN, CN, silt, clay	10	18.47	0.62	18.60
	Elevation, aspect, TPI, NDVI, GNDVI, NDMI, temperature, moisture, bulk density, NO_3-N, NH_4-N, DOC, TDN, SOC, SN, CN, silt, clay	10	18.48	0.63	18.60
	Elevation, aspect, TPI, NDVI, GNDVI, NDMI, temperature, moisture, bulk density, NO_3-N, NH_4-N, DOC, TDN, SOC, SN, CN, silt	9	18.47	0.63	18.60
	Elevation, aspect, TPI, NDVI, GNDVI, NDMI, temperature, moisture, bulk density, NO_3-N, NH_4-N, DOC, TDN, SOC, SN, CN	9	18.48	0.63	18.60
	Elevation, aspect, TPI, NDVI, GNDVI, NDMI, temperature, moisture, NO_3-N, NH_4-N, DOC, TDN, SOC, SN, CN	8	18.48	0.64	18.61
	Elevation, aspect, NDVI, GNDVI, NDMI, temperature, moisture, NO_3-N, NH_4-N, DOC, TDN, SOC, SN, CN	8	18.48	0.64	18.61
	Elevation, aspect, NDVI, GNDVI, NDMI, temperature, moisture, NO_3-N, NH_4-N, DOC, TDN, SOC, CN	7	18.49	0.65	18.62
	Elevation, aspect, NDVI, GNDVI, NDMI, temperature, moisture, NO_3-N, DOC, TDN, SOC, CN	7	18.49	0.65	18.62
	Elevation, NDVI, GNDVI, NDMI, temperature, moisture, NO_3-N, DOC, TDN, SOC, CN	6	18.48	0.65	18.61
	Elevation, NDVI, GNDVI, NDMI, temperature, moisture, NO_3-N, TDN, SOC, CN	6	18.49	0.65	18.62
	NDVI, GNDVI, NDMI, temperature, moisture, NO_3-N, TDN, SOC, CN	5	18.49	0.66	18.62
	NDVI, GNDVI, NDMI, moisture, NO_3-N, TDN, SOC, CN	5	18.49	0.66	18.62
	NDVI, GNDVI, NDMI, moisture, NO_3-N, TDN, CN	4	18.51	0.68	18.63
	NDVI, GNDVI, NDMI, moisture, TDN, CN	6	18.51	0.68	18.63
	GNDVI, NDMI, moisture, TDN, CN	5	18.51	0.68	18.63
	GNDVI, NDMI, TDN, CN	3	18.52	0.69	18.64
	GNDVI, NDMI, TDN	3	18.55	0.72	18.65
	GNDVI, NDMI	2	18.45	0.63	18.59
	GNDVI	2	18.31	0.51	18.51

Table B6: The minimum, maximum, mean, standard deviation, and standard error of the measured fluxes at all the sampling points and the predicted landscape fluxes using remote sensing (RS), soil properties (SP), and combined data (CD).

Measured fluxes at sampling points		**Summer**					**Autumn**				
Land use	**Flux type**	**Min**	**Max**	**Mean**	**STDEV**	**SE**	**Min**	**Max**	**Mean**	**STDEV**	**SE**
Forest	SR/ER-CO_2-C (mg m^{-2} h^{-1})	60	589	210	111	12.0	10	446	74	53	5.5
Grassland		136	693	350	123	14.1	9	419	131	82	8.6
Arable		78	877	431	192	23.3	14	238	84	51	6.1
Forest	CH_4-C (µg m^{-2} h^{-1})	-201	176	-62	47	5.1	-214	7	-68	48	4.9
Grassland		-84	221	-9	43	5.2	-100	28	-23	21	2.4
Arable		-133	157	8	74	12.3	-43	11	-17	10	1.4
Forest	N_2O-N (µg m^{-2} h^{-1})	-13	117	14	24	2.9	-17	78	5	11	1.3
Grassland		-17	281	32	57	7.0	-18	154	12	30	3.7
Arable		13	282	84	65	8.4	-15	54	12	12	1.6
Predicted landscape fluxes (RS data)											
Forest	SR/ER-CO_2-C (mg m^{-2} h^{-1})	37	327	171	51	0.03	38	288	74	26	0.01
Grassland		59	484	294	70	0.10	39	477	186	89	0.13
Arable		35	668	324	111	0.08	28	559	102	86	0.06
Forest	CH_4-C (µg m^{-2} h^{-1})	-147	65	-70	21	0.01	-148	65	-72	25	0.01
Grassland		-60	50	-15	17	0.02	-64	32	-18	11	0.02
Arable		-60	89	-5	23	0.02	-60	75	-16	11	0.01
Forest	N_2O-N (µg m^{-2} h^{-1})	-8	38	7	5	0.003	-6	27	4	4	0.002
Grassland		-8	144	26	34	0.05	-9	69	12	8	0.01
Arable		0	190	60	33	0.02	-1	183	18	17	0.01
Predicted landscape fluxes (SP data)											
Forest	SR/ER-CO_2-C (mg m^{-2} h^{-1})	55	343	194	34	0.02	41	214	70	14	0.01
Grassland		72	470	320	38	0.05	52	319	128	44	0.06
Arable		36	733	266	90	0.06	28	733	124	60	0.04
Forest	CH_4-C (µg m^{-2} h^{-1})	-123	54	-51	11	0.01	-138	-29	-51	10	0.01
Grassland		-65	37	-8	8	0.01	-65	13	-10	6	0.01
Arable		-87	85	-7	26	0.02	-67	85	-13	17	0.01
Forest	N_2O-N (µg m^{-2} h^{-1})	-9	49	9	7	0.00	-9	23	6	4	0.00
Grassland		-6	124	20	8	0.01	-7	54	7	7	0.01
Arable		12	157	45	10	0.01	0	150	19	9	0.01
Predicted landcsape fluxes (CD data)											
Forest	SR/ER-CO_2-C (mg m^{-2} h^{-1})	82	325	185	31	0.02	42	195	66	14	0.01
Grassland		155	496	322	47	0.07	52	349	145	61	0.09
Arable		68	694	321	105	0.08	29	568	110	59	0.04
Forest	CH_4-C (µg m^{-2} h^{-1})	-125	55	-57	18	0.01	-136	-27	-59	19	0.01
Grassland		-69	36	-6	9	0.01	-69	13	-11	6	0.01
Arable		-72	78	0	24	0.02	-72	53	-17	11	0.01
Forest	N_2O-N (µg m^{-2} h^{-1})	-9	49	9	7	0.00	-9	23	6	4	0.00
Grassland		-9	152	25	31	0.05	-8	83	6	7	0.01
Arable		16	168	58	21	0.02	1	128	16	12	0.01

Table B7: Description of the sampling locations within the common hotspot patches of all three GHG fluxes.

Site ID	Land use	Site description and observed soil properties
Q10	Forest	Riparian forest with alder (*Alnus*) trees, higher soil moisture, nitrate, ammonium and DOC concentrations
Q73	Grassland	Riparian grassland with higher soil moisture, ammonium and DOC concentrations
Q80	Grassland	Riparian grassland with Clover (*Trifolium*) and higher soil moisture
C23	Grassland	Higher soil moisture, nitrate, ammonium and DOC concentrations
C79	Grassland	Higher ammonium and DOC concentrations
C45	Grassland	A lot of Clover (*Trifolium*)
C37	Grassland	A lot of Clover (*Trifolium*)
E7	Grassland	A lot of Clover (*Trifolium)*
C3	Arable land	Barley crops
C13	Arable land	Barley crops and the soils had higher nitrate concentrations
Q20	Arable land	Barley crops
C12	Arable land	Barley crops and the soils had higher soil moisture
C56	Arable land	Wheat crops and the soils had higher soil moisture
C97	Arable land	Wheat crops and the soils had higher nitrate concentrations

589 **Acknowledgments**

This work was part of the MINCA (MItigation of Nitrogen pollution at CAtchment scale) research project. The authors gratefully acknowledge the German Research Foundation (DFG) for funding the project (HO6420/1-1, KR5265/1-1). KBB additionally received funds via the Pioneer Center for Research in Sustainable Agricultural Futures (Land-CRAFT), DNRF Grant Number P2. Furthermore, Wangari, E. received doctoral funding from the German Academic Exchange Service (DAAD).

590 **Declaration of competing interest**

The authors declare that they have no conflict of interest.

591 **Author contribution**

Conceptualization: KB, LB, GG, TH, RK, DK, EW. Field measurements and laboratory work: EW, RM, TH. Data analysis: EW, RM, KB. Funding acquisition: KB, RK, TH, DK. Writing-original draft preparation: EW, RM, KB. Writing-final draft: EW, KB, RM, LB, RK, TH, DK, GG.

592 **Data availability**

The data will be made freely available via the Zenodo repository after publishing. However, reviewers can request the data anytime during the review process, and the corresponding author will provide it via email.

References

Adjuik, T. A., & Davis, S., C.: Machine learning approach to simulate soil CO_2 fluxes under cropping systems. Agronomy, 12, 197, https://doi.org/10.3390/ agronomy12010197, 2022.

Arias-Navarro, C., Diaz-Pines, E., Klatt, S., Brandt, P., Rufino, M. C., Butterbach-Bahl, K., & Verchot, L. V.: Spatial variability of soil N_2O and CO_2 fluxes in different topographic positions in a tropical montane forest in Kenya. Journal of Geophysical Research: Biogeosciences, 3 (122), 514–527, https://doi.org/10.1002/2016JG003667, 2017.

Bannari, A., Morin, D., Bonn, F., & Huete, A., R.: A review of vegetation indices. Remote Sensing Reviews, 13 (1-2), 95-120, DOI: 10.1080/02757259509532298, 1995.

Barton L., McLay C. D. A., Schipper L. A., & Smith C. T.: Annual denitrification rates in agricultural and forest soils: a review. Australian Journal of Soil Research, 37 (6), 1073 – 1094, https://doi.org/10.1071/SR99009, 1999.

Berrar, D.: Cross-validation. Encyclopedia of Bioinformatics and Computational Biology, 1, 542-545, DOI: 10.1016/B978-0-12-809633-8.20349-X, 2018.

Breiman, L.: Random Forests. Machine Learning, 45, 5–32, http://dx.doi.org/10.1023/A:1010933404324, 2001.

Butterbach-Bahl, K., & Dannenmann, M.: Denitrification and associated soil N_2O emissions due to agricultural activities in a changing climate. Current Opinion in Environmental Sustainability, 3, (5), 389-395, DOI 10.1016/j.cosust.2011.08.004, 2011.

Butterbach-Bahl, K., Baggs, E. M., Dannenmann, M., Kiese, R., & Zechmeister-Boltenstern, S.: Nitrous oxide emissions from soils: How well do we understand the processes and their controls? Philosophical Transactions of the Royal Society B: Biological Sciences, *368* (1621), 20130122, https://doi.org/10.1098/rstb.2013.0122, 2013.

Butterbach-Bahl, K., Gettel, G., Kiese, R., Fuchs, K., Werner C., Rahimi, J., Barthel, M., & Merbold, L.: Livestock enclosures in drylands of Sub-Saharan Africa are overlooked hotspots of N_2O emissions. Nature Communications, 11, 4644, https://doi.org/10.1038/s41467-020-18359-y, 2020.

Ciarlo, E., Conti, M., Bartoloni, N.: The effect of moisture on nitrous oxide emissions from soil and the $N_2O/(N_2O+N_2)$ ratio under laboratory conditions. Biology and Fertility of Soils, 43, 675–681, https://doi.org/10.1007/s00374-006-0147-9, 2007.

Congedo, L.: Semi-Automatic Classification Plugin: A Python tool for the download and processing of remote sensing images in QGIS. Journal of Open Source Software, 6 (64), p.3172, DOI: 10.21105/joss.03172, 2021.

Dutaur, L., & Verchot, L.: A global inventory of the soil CH_4 sink. Global Biogeochemical Cycles, 21 (4), GB4013, https://doi.org/10.1029/2006GB002734, 2007.

Dhakal, S., J.C. Minx, F.L. Toth, A. Abdel-Aziz, M.J. Figueroa Meza, K. Hubacek, I.G.C. Jonckheere, Yong-Gun Kim, G.F. Nemet, S. Pachauri, X.C. Tan, T. Wiedmann.: Emissions Trends and Drivers, in: IPCC, 2022: Climate Change 2022: Mitigation of Climate Change. Contribution of Working Group III to the Sixth Assessment Report of the Intergovernmental Panel on Climate Change [P.R. Shukla, J. Skea, R. Slade, A. Al Khourdajie, R. van Diemen, D. McCollum, M. Pathak, S. Some, P. Vyas, R. Fradera, M. Belkacemi, A. Hasija, G. Lisboa, S. Luz, J. Malley, (eds.)]. Cambridge University Press, Cambridge, UK and New York, NY, USA. doi: 10.1017/9781009157926.004, 2022.

Dorich, C. D., De Rosa, D., Barton, L., Grace, P., Rowlings, D., Migliorati, M. A., et al.: Global Research Alliance N_2O chamber methodology guidelines: Guidelines for gap-filling missing measurements. Journal of Environmental Quality, 49 (5),1186-1202, doi: 10.1002/jeq2.20138, 2020.

Gao, B.: NDWI-A Normalized Difference Water Index for Remote Sensing of vegetation liquid water from space. Remote Sensing of Environment, 58 (3), 257-266, DOI: 10.1016/S0034-4257(96)00067-3, 1196.

Gitelson, A., A., & Merzlyak, M., N.: Remote sensing of chlorophyll concentration in higher plant leaves. Advances in Space Research, 22 (5), 689-692, https://doi.org/10.1016/S0273-1177 (97) 01133-2, 1998.

Gradka, R., & Kwinta, A.: A short review of interpolation methods used for terrain modeling. Geomatics, Land Management and Landscape, 4, 29–47, https://doi.org/10.15576/GLL/2018.4.29, 2018.

Groffman, P., M., & Tiedje, J., M.: Denitrification in north temperate forest soils: Spatial and temporal patterns at the landscape and seasonal scales. Soil Biology and Biochemistry, 21(5), 613–620, https://doi.org/https://doi.org/10.1016/0038-0717(89)90053-9, (1989).

Haas, E., Klatt, S., Fröhlich, A., Kraft, P., Werner, C., Kiese, R., Grote, R., Breuer, L., & Butterbach-Bahl, K.: A process model for simulation of biosphere-atmosphere-hydrosphere exchange processes at site and landscape scale. Landscape Ecology, 28, 615–636, https://doi.org/10.1007/s10980-012-9772-x, 2013.

Hagedorn, F., & Bellamy, P.: Hot spots and hot moments for greenhouse gas emissions from soils, in Soil Carbon in Sensitive European Ecosystems: From Science to Land Management, edited by: Jandl, R., Rodeghiero, M., and Olsson, M., 13–32, Wiley-Blackwell, Chichester, UK. https://doi.org/10.1002/9781119970255.ch2, 2011.

Hamrani, A., Akbarzadeh, A., Madramootoo, C. A.: Machine learning for predicting greenhouse gas emissions from agricultural soils. Science of The Total Environment, 741, 140338, DOI: 10.1016/j.scitotenv.2020.140338, 2020.

Han, L., Yu, G.-R., Chen, Z., Zhu, X.-J., Zhang, W.-K., Wang, T.-J., et al.: Spatiotemporal pattern of ecosystem respiration in China estimated by integration of machine learning with ecological understanding. Global Biogeochemical Cycles, (11), 36, e2022GB007439, https://doi. org/10.1029/2022GB007439, 2022.

Hassan, M. U., Aamer, M., Mahmood, A., Awan, M. I., Barbanti, L., Seleiman, M. F., Bakhsh, G., Alkharabsheh, H. M., Babur, E., Shao, J., et al.: Management Strategies to Mitigate N_2O Emissions in Agriculture. Life, 12, 439. https://doi.org/10.3390/life12030439, 2022.

Hensen, A., Skiba, U., & Famulari, D.: Low cost and state of the art methods to measure nitrous oxide emissions. Environmental Research Letters, 8 (10), 025022, https://doi.org/10.1088/1748-9326/8/2/025022, 2013.

IPCC.: Summary for policymakers. In P. R. Shukla, J. Skea, E. Calvo Buendia, V. Masson-Delmotte, H.-O. Portner, D. C. Roberts, et al. (Eds.), Climate change and land: An IPCC special report on climate change, desertification, land degradation, sustainable land management, food security, and greenhouse gas fluxes in terrestrial ecosystem, 2019.

Jian, J., Steele, M. K., Thomas, R. Q., Day, S. D., & Hodges, S. C.: Constraining estimates of global soil respiration by quantifying sources of variability. Global Change Biology, 24 (9), 4143–4159, https://doi.org/10.1111/gcb.14301, 2018.

Joshi, D. R., Clay, D. E., Clay, S. A., Moriles-Miller, J., Daigh, A. L., Reicks, G., Westhoff, S.: Quantification and Machine learning based N_2O-N and CO_2-C emissions predictions from a decomposing rye cover crop. Agronomy Journal, https://doi.org/10.1002/agj2.21185, 2022.

Kaiser, K. E., McGlynn, B. L., & Dore, J. E.: Landscape analysis of soil methane flux across complex terrain. Biogeosciences, 15, 3143–3167, https://doi.org/10.5194/bg-15-3143-2018, 2018.

Koch, J., Elsgaard, L., Greve, M.H., Gyldenkærne, S., Hermansen, C., Levin, G., Wu, S., & Stisen, S.: Water table driven greenhouse gas emission estimate guides peatland restoration at national scale. Biogeosciences, 20, 2387–2403, https://doi.org/10.5194/bg-20-2387-2023, 2023.

Kuhn, M.: Building Predictive Models in R Using the caret Package. Journal of Statistical Software, 28, (5), 1-26, DOI: 10.18637/jss.v028.i05, 2008.

Le Mer, J., & Roger, P. A.: Production, oxidation, emission and consumption of methane by soils: A review. European Journal of Soil Biology, 1(37), 25–50, https://doi.org/10.1016/S1164-5563(01)01067-6, 2001.

Levy, P., Clement, R., Cowan, N., Keane, B., Myrgiotis, V., van Oijen, M., et al.: Challenges in scaling up greenhouse gas fluxes: Experience from the UK greenhouse gas emissions and feedbacks program. Journal of Geophysical Research: Biogeosciences, 127, e2021JG006743, https://doi.org/10.1029/2021JG006743, 2022.

Malakhov, D. V., & Tsychuyeva, Y. T.: Calculation of the biophysical parameters of vegetation in an arid area of south-eastern Kazakhstan using the normalized difference moisture index (NDMI). Cent. Asian J. Environ. Sci. Technol. Innov., 1 (4), 189-198, DOI: 10.22034/CAJESTI.2020.04.01, 2020.

Malique, F., Ke, P., Boettcher, J., Dannenmann, M., & Butterbach-Bahl, K.: Plant and soil effects on denitrification potential in agricultural soils. Plant Soil, 439 (1–2), 459–474, https://doi.org/10.1007/s11104-019-04038-5, 2019.

Mason, C. W., Stoof, C. R., Richards, B. R, Das, S., & Goodale, C. L.: Hotspots of Nitrous Oxide Emission in Fertilized and Unfertilized Perennial Grasses. Soil Science Society of American Journal, 81, (3), 450-458, DOI: 10.2136/sssaj2016.08.0249, 2017.

McDaniel, M. D., Simpson, R. G., Malone, B. P., McBratney, A. B., Minasny, B., & Adams, M. A.: Quantifying and predicting spatio-temporal variability of soil CH_4 and N_2O fluxes from a seemingly homogeneous Australian agricultural field. Agriculture, Ecosystems and Environment, 240, 182-193, http://dx.doi.org/10.1016/j.agee.2017.02.017, 2017.

Meyer, H. and Pebesma, E.: Machine learning-based global maps of ecological variables and the challenge of assessing them. Nature Communications, 13, 2208, https://doi.org/10.1038/s41467-022-29838-9, 2022.

Molodovskaya, M., Warland, J., Richards, B. K., Öberg, G., & Steenhuis, T. S.: Nitrous oxide from heterogeneous agricultural landscapes: Source contribution analysis by eddy covariance and chambers. Soil Science Society of American Journal, 75, (5), 1829-1838, https://doi.org/10.2136/sssaj2010.0415, 2011.

Oertel, C., Matschullat, J., Zurba, K., Zimmermann, F., & Erasmi, S.: Greenhouse gas emissions from soils - a review. Geochemistry, 763 (3), 327–352, https://doi.org/10.1016/j.chemer.2016.04.002, 2016.

Philibert, A., Loyce, C., & Makowski, D.: Prediction of N_2O emission from local information with Random Forest. Environmental Pollution, 177, 156-63, doi: 10.1016/j.envpol.2013.02.019, 2013.

Räsänen, A., Manninen, T., Korkiakoski, M., Lohila, A., & Virtanen, T.: Predicting catchment-scale methane fluxes with multi-source remote sensing. Landscape Ecology, 36, 1177–1195, https://doi.org/10.1007/s10980-021-01194-x, 2021.

Rosenstock, T. S., Mariana, C. R., Chirinda, N., van Bussel, L., Reidsma, P., & Butterbach-Bahl, K.: Scaling point and plot measurements of greenhouse gas fluxes, balances, and intensities to whole farms and landscapes. In: Rosenstock, T. S., Mariana, C. R., Butterbach-Bahl, K. Wollenberg, L., & Richards, M. (Eds). 2016. Methods for Measuring Greenhouse Gas Balances and Evaluating Mitigation Options in Smallholder Agriculture. Springer, Switzerland. pp.175-188, 2016.

Saha, D., Basso, B., & Robertson, G. P.: Machine learning improves predictions of agricultural nitrous oxide (N_2O) emissions from intensively managed cropping systems. Environmental Research Letters, 16, (2), 024004, https://doi.org/10.1088/1748-9326/abd2f3, 2021.

Sahraei, A., Kraft, P., Windhorst, D., & Breuer, L.: High-Resolution, in situ monitoring of stable isotopes of water revealed insight into hydrological response behavior. Water, 12 (2), 565, https://doi.org/10.3390/w12020565, 2020.

Sahraei, A., Houska, T., & Breuer, L.: Deep learning for isotope hydrology: The application of long short-term memory to estimate high temporal resolution of the stable isotope concentrations in stream and groundwater. Frontiers in Water, 3, 113, https://doi.org/10.3389/frwa.2021.740044, 2021.

Steinkamp, R., Butterbach-Bahl, K., & Papen, H.: Methane oxidation by soils of an N-limited and N-fertilized spruce forest in the Black Forest, Germany. Soil Biology and Biochemistry, 33(2), 145–153, https://doi.org/10.1016/S0038-0717(00)00124-3, 2000.

Sundqvist, E., Persson, A., Kljun, N., Vestin, P., Chasmer, L., Hopkinson, C., & Lindroth, A.: Upscaling of methane exchange in a boreal forest using soil chamber measurements and high-resolution LiDAR elevation data. Agricultural and Forest Meteorology, 15(214– 215), 393–401, https://doi.org/10.1016/j.agrformet.2015.09.003, 2015.

Tian, H., Xu, R., Canadell, J. G., Thompson, R. L., Winiwarter, W., Suntharalingam, P., et al.: A comprehensive quantification of global nitrous oxide sources and sinks. Nature, 586(7828), 248–256, https://doi.org/10.1038/s41586-020-2780-0, 2020.

Tiemeyer, B., Freibauer, A., Borraz, E. A., Augustin, J., Bechtold, M., Beetz, S., et al.: A new methodology for organic soils in national greenhouse gas inventories: Data synthesis, derivation and application. Ecological Indicators, 109, 105838, https://doi.org/10.1016/j.ecolind.2019.105838, 2020.

Tubiello, F. N., Salvatore, M., Rossi, S., Ferrara, A., Fitton, N., & Smith, P.: The FAOSTAT database of greenhouse gas emissions from agriculture. Environmental Research Letters, 8 (1), [015009], https://doi.org/10.1088/1748-9326/8/1/015009, 2013.

Vainio, E., Peltola, O., Kasurinen, V., Kieloaho, A, Tuittila, E, Pihlatie, M.: Topography-based statistical modelling reveals high spatial variability and seasonal emission patches in forest floor methane flux. Biogeosciences, 18 (6), 2003–2025, https://doi.org/10.5194/bg-18-2003-2021, 2021.

van Kessel, C., Pennock, D. & Farrell, R.: Seasonal variations in denitrification and nitrous oxide evolution at the landscape scale. Soil Sci. Soc. Am. J. 57, 988–995, doi:10.2136/sssaj1993.03615995005700040018x, 1993.

Wagner-Riddle, C., Baggs, E. M., Clough, T. J., Fuchs, K., & Petersen, S. O.: Mitigation of nitrous oxide emissions in the context of nitrogen loss reduction from agroecosystems: managing hot spots and hot moments. Current Opinion in Environmental Sustainability, (47), 46-53, https://doi.org/10.1016/j.cosust.2020.08.002, 2020.

Wangari, E. G., Mwanake, R. M., Kraus, D., Werner, C., Gettel, G. M., Kiese, R., Breuer, L., Butterbach-Bahl, K., & Houska, T.: Number of Chamber Measurement Locations for Accurate Quantification of Landscape-Scale Greenhouse Gas Fluxes: Importance of Land Use, Seasonality, and Greenhouse Gas Type. Journal of Geophysical Research: Biogeosciences, 127 (9), e2022JG006901, https://doi.org/10.1029/2022JG006901, 2022.

Warner, D. L., Guevara, M., Inamdar, S., & Vargas, R.: Upscaling soil-atmosphere CO_2 and CH_4 fluxes across a topographically complex forested landscape. Agricultural and Forest Meteorology, 264, 80–91, https://doi.org/10.1016/j.agrformet.2018.09.020, 2019.

Webster, K. L., Creed, F., Beall, F. D., & Bourbonnie`re, R. A.: Sensitivity of catchment-aggregated estimates of soil carbon dioxide efflux to topography under different climatic conditions. Journal of geophysical research, 113, G03040, doi:10.1029/2008JG000707, 2008.

Zhang, C., Comas, X., & Brodylo, D.: A remote sensing technique to upscale methane emission flux in a subtropical peatland. Journal of Geophysical Research: Biogeosciences, 125, e2020JG006002, https://doi.org/10.1029/2020JG00600, 2020.

Plain text summary

Agricultural landscapes act as sinks or sources of the greenhouse gases (GHG) CO_2, CH_4 or N_2O. Fluxes of these GHGs between ecosystems and the atmosphere are controlled by various physico-chemical and biological processes. Therefore, fluxes depend on environmental conditions such as moisture, temperature, or soil parameters, which results in large spatial and temporal variations of GHG fluxes. Here we describe an example how this variation may be studied and analyzed.